8504 *Inorg. Chem.* **2010**, *49*, 8504–8523
DOI: 10.1021/ic101152x

Inorganic Chemistry
Article

X-ray Crystal Structures of $[XeF][MF_6]$ (M = As, Sb, Bi), $[XeF][M_2F_{11}]$ (M = Sb, Bi) and Estimated Thermochemical Data and Predicted Stabilities for Noble-Gas Fluorocation Salts using Volume-Based Thermodynamics

Hugh St. A. Elliott,[†] John F. Lehmann,[†] Hélène P.A. Mercier,[†] H. Donald Brooke Jenkins,*[,‡] and Gary J. Schrobilgen*[,†]

[†]*Department of Chemistry, McMaster University, Hamilton, Ontario, L8S 4M1, Canada, and*
[‡]*Department of Chemistry, University of Warwick, Coventry, West Midlands CV4 7AL, U.K.*

Received June 8, 2010

The crystal structures of the xenon(II) salts, $[XeF][SbF_6]$, $[XeF][BiF_6]$, and $[XeF][Bi_2F_{11}]$, have been determined for the first time, and those of XeF_2, $[XeF][AsF_6]$, $[XeF][Sb_2F_{11}]$, and $[XeF_3][Sb_2F_{11}]$ have been redetermined with greater precision at −173 °C. The $Bi_2F_{11}^-$ anion, which has a structure analogous to those of the $As_2F_{11}^-$ and $Sb_2F_{11}^-$ anions, has been structurally characterized by single crystal X-ray diffraction for the first time as its XeF^+ salt. The fluorine bridge between the bismuth atoms is asymmetric with Bi- - -F_b bond lengths of 2.092(6) and 2.195(6) Å and a Bi- - -F_b′- - -Bi bridge bond angle of 145.3(3)°. The XeF^+ cations interact with their anions by means of Xe- - -F_b- - -M bridges. Consequently, the solid-state Raman spectra of $[XeF][MF_6]$ (M = As, Sb, Bi) were modeled as the gas-phase ion pairs and assigned with the aid of quantum-chemical calculations. Relationships among the terminal Xe−F_t and bridge Xe- - -F_b bond lengths and stretching frequencies and the gas-phase fluoride ion affinities of the parent Lewis acid that the anion is derived from are considered. The analogous krypton ion pairs, $[KrF][MF_6]$ (M = As, Sb, Bi) were also calculated and compared with their previously published X-ray crystal structures. The calculated cation−anion charge separations indicate that the $[XeF][MF_6]$ salts are more ionic than their krypton analogues and that XeF_2 is a stronger fluoride ion donor than KrF_2. The lattice energies, standard enthalpies, and free energies of formation for salts containing the NgF^+, $Ng_2F_3^+$, XeF_3^+, XeF_5^+, $Xe_2F_{11}^+$, and $XeOF_3^+$ (Ng = Ar, Kr, Xe) cations were estimated using volume-based thermodynamics (VBT) based on crystallographic and estimated ion volumes. These estimated parameters were then used to predict the stabilities of noble-gas salts. VBT is used to examine and predict the stabilities of, inter alia, the salts $[XeF_m][Sb_nF_{5n+1}]$ and $[XeF_m][As_nF_{5n+1}]$ (m = 1, 3; n = 1, 2). VBT also confirms that XeF^+ salts are stable toward redox decomposition to Ng, F_2, and MF_5 (M = As, Sb), whereas the isolable krypton compounds and the unknown ArF^+ salts are predicted to be unstable by VBT with the ArF^+ salts being the least stable.

Introduction

The low-temperature X-ray crystal structures of $[KrF][MF_6]$ (M = As, Sb, Bi, Au)[1,2] have been previously determined in this laboratory and were used to investigate structural relationships among this series of salts and their vibrational spectra. In contrast and although numerous XeF^+ salts have been synthesized since the discovery of noble-gas reactivity in 1962,[3−6] the only XeF^+ salts for which X-ray crystal structures had been determined at the onset of the present work were those of $[XeF][RuF_6]$,[7] $[XeF][AsF_6]$,[8] and $[XeF][Sb_2F_{11}]$.[9,10] Other than the crystal structure of $[XeF][RuF_6]$, the remaining structures were of lower precision than those of the $[KrF][MF_6]$ (M = As, Sb, Bi) salts.[1] In the present work, the low-temperature (−173 °C) X-ray

*To whom correspondence should be addressed. E-mail: schrobil@mcmaster.ca (G.J.S., syntheses, crystallography and quantum-chemical calculations), h.d.b.jenkins@warwick.ac.uk (H.D.B.J., volume-based thermodynamics).

(1) Lehmann, J. F.; Dixon, D. A.; Schrobilgen, G. J. *Inorg. Chem.* **2001**, *40*, 3002–3017.
(2) Lehmann, J. F.; Schrobilgen, G. J. *J. Fluorine Chem.* **2003**, *119*, 109–124.
(3) Selig, H.; Holloway, J. H. *Top. Curr. Chem.* **1984**, *124*, 33–90.
(4) Žemva, B. *Croat. Chem. Acta* **1988**, *61*, 163–187.
(5) Schrobilgen, G. J. Noble Gas Chemistry. In *Encyclopedia of Physical Science and Technology*, 3rd ed.; Hawthorne, M.F., Ed.; Academic Press: San Diego, CA, 2002; Vol. *10*, pp 449−461.
(6) Schrobilgen, G. J.; Moran, M. D. Noble Gas Compounds. In *Kirk-Othmer Encyclopedia of Chemical Technology*, 5th ed.; John Wiley & Sons, Inc.: Hoboken, NJ, 2006; Chapter 17, pp 323−343.
(7) Bartlett, N.; Gennis, M.; Gibler, D. D.; Morrell, B. K.; Zalkin, A. *Inorg. Chem.* **1973**, *12*, 1717–1721.
(8) Zalkin, A.; Ward, D. L.; Biagioni, R. N.; Templeton, D. H.; Bartlett, N. *Inorg. Chem.* **1978**, *17*, 1318–1322.
(9) McRae, V. M.; Peacock, R. D.; Russell, D. R. *Chem. Commun.* **1969**, 62–63.
(10) Burgess, J.; Fraser, C. J. W.; Mc Rae, V. M.; Peacock, R. D.; Russell, D. R. In *Herbert H. Hyman Memorial Volume. J. Inorg. Nucl. Chem.* **1976**, (No Supplement Available), 183–188.

Published on Web 08/24/2010

crystal structures of $[XeF][SbF_6]$, $[XeF][BiF_6]$, and $[XeF][Bi_2F_{11}]$ have been determined for the first time and those of $[XeF][AsF_6]$, $[XeF][SbF_6]$, and $[XeF][Sb_2F_{11}]$ have been redetermined at higher precisions. By so doing, the standard deviations of the $Xe-F_t$ and $Xe\text{---}F_b$ bond lengths have been brought into line with those of the $[KrF][MF_6]$ salts[1] so that meaningful comparisons with the geometric parameters of KrF^+ and XeF^+ salts can now be made. As a result, possible relationships among the Xe−F bond lengths, their stretching frequencies, and the fluoride ion affinities of the parent Lewis acids may also be examined.

With the exception of the neutral noble-gas compounds, KrF_2, XeF_2, XeF_4, XeF_6, $XeOF_4$, XeO_3, and XeO_4, which have been successfully studied by calorimetric methods,[6,11] the thermochemistry of noble-gas compounds has generally been a neglected area of study. The paucity of thermodynamic information on the noble-gas cations is particularly noteworthy. Compounds that were originally formulated as Lewis acid adducts of neutral fluorides and oxide fluorides, were subsequently shown to be better described as salts containing the NgF^+, $Ng_2F_3^+$, XeF_3^+, XeF_5^+, $Xe_2F_{11}^+$, and $XeOF_3^+$ (Ng = Kr, Xe) cations.[3−6] All had been prepared within several years of Bartlett's discovery of noble-gas reactivity in 1962.[12] His discovery showed that PtF_6 oxidized xenon to a compound Bartlett assigned as having the ionic formulation "$[Xe][PtF_6]$". This compound was subsequently reformulated as a XeF^+ salt, $[XeF][PtF_6]$, in admixture with PtF_5 which, when warmed to ≤60 °C, gave $[XeF][Pt_2F_{11}]$.[13,14] The mixture of $[XeF][PtF_6]$ and PtF_5 is presumed to result from the reaction of initially formed "$[Xe][PtF_6]$" with PtF_6.

Although calorimetric methods are well established and are generally the preferred method of obtaining thermodynamic information, the thermodynamic instability and/or potent oxidizing properties of noble-gas containing compounds present a formidable obstacle to obtaining reproducible and reliable data. Consequently, experimental results are scarce for the noble-gas containing salts. The only experimental enthalpies of reaction that have been measured for XeF^+ salts are for reactions of XeF_2 with $M'F_5$ (M′ = Sb, Nb, Ta) that give $[XeF][M'F_6]$ and $[XeF][M'_2F_{11}]$[15] and $[XeF][Sb_2F_{11}]$.[10] Several studies have shown that lattice enthalpies, enthalpies of formation, and free energies of formation for inorganic systems can be obtained from ion volumes derived from crystallographic methods.[16−20] Although the use of volume-based thermodynamics (VBT) in this paper may use thermodynamic and other data which may be less certain than experimentally determined values, the VBT approach, as implemented in the present study, illustrates the considerable ground that can be covered by employing this simple approach (see Supporting Information) which needs no sophisticated software to substantiate observed chemical behavior and to predict the feasibility of preparing yet unknown noble-gas compounds.

Results and Discussion

Syntheses of $[XeF][MF_6]$ (M = As, Sb, Bi) and $[XeF][M_2F_{11}]$ (M = Sb, Bi). Xenon difluoride acts as a fluoride ion donor toward the strong Lewis acids AsF_5,[8,21] SbF_5,[9,10,21] and BiF_5.[22] The $[XeF][MF_6]$ (M = As, Sb, Bi) salts were prepared by dissolving 1:1 molar ratios of XeF_2 and the appropriate pnictogen pentafluoride in anhydrous HF (aHF) solvent. Crystals of these salts were obtained by slowly cooling the HF solutions, followed by the removal of the solvent as previously described.[2]

The $[XeF][Sb_2F_{11}]$ salt was prepared by the direct reaction of XeF_2 with excess SbF_5.[23] Single crystals were obtained by allowing an SbF_5 solution of the salt to cool from 45 °C to ambient temperature over the course of several days. The salt, $[XeF][Bi_2F_{11}]$, was prepared by allowing a 1:2 molar ratio of XeF_2 and BiF_5 to react in anhydrous HF (aHF) solvent.[22] Crystals suitable for a X-ray structure determination were obtained by slow removal of the solvent under vacuum at −48 °C. An attempt to isolate crystalline $[XeF][Bi_2F_{11}]$ by slowly cooling a dilute HF solution containing a 2:1 molar ratio of BiF_5/XeF_2 resulted in the isolation of crystalline $[XeF][BiF_6]$, which is consistent with an equilibrium between $Bi_2F_{11}^-$ and BiF_5/BiF_6^- (eq 1) that shifts to the right

$$Bi_2F_{11}^- \rightleftharpoons BiF_5 + BiF_6^- \quad (1)$$

when the solution concentration is low. The isolation of $[XeF][BiF_6]$ under dilute conditions is also expected to be favored by its lower solubility relative to that of $[XeF][Bi_2F_{11}]$. The greater lattice energy calculated for $[XeF][BiF_6]$ (536 kJ mol^{-1}) compared to that of $[XeF][Bi_2F_{11}]$ (471 kJ mol^{-1}) (see Thermochemistry, Table 6, and Supporting Information) presumably also contributes to the lower solubility of $[XeF][BiF_6]$ and its preferential crystallization.

Attempts to prepare $[XeF][As_2F_{11}]$ by the reaction of $[XeF][AsF_6]$ with a 15-fold molar excess of liquid AsF_5 at −30 and −78 °C, and by the reaction of a 15-fold molar excess of AsF_5 dissolved in aHF (50/50 v/v) at −40 °C were unsuccessful. Such attempts were monitored by recording the Raman spectrum of the XeF^+ salt under the frozen solvent medium at −160 °C. The inability to isolate $[XeF][As_2F_{11}]$ under these conditions contrasts with the ability to isolate the analogous $[XeF][Sb_2F_{11}]$ and $[XeF][Bi_2F_{11}]$ salts, and is consistent with volume-based thermodynamic calculations (see Thermochemistry of Noble-Gas Fluorocation Salts, section (f) (i)). Although cryoscopic[24]

(11) Bartlett, N.; Sladky, F. O. In *Comprehensive Inorganic Chemistry*, 1st ed.;Trotman-Dickenson, A. F., Ed.; Pergamon Press Ltd.: Oxford, U.K., 1973; Vol. *1*, Chapter 6, pp 213−330.
(12) Bartlett, N. *Proc. Chem. Soc.* **1962**, 218.
(13) Sladky, F. O.; Bulliner, P. A.; Bartlett, N. *J. Chem. Soc. A* **1969**, 2179–2188.
(14) Graham, L.; Graudejus, O.; Jha, N. K.; Bartlett, N. *Coord. Chem. Rev.* **2000**, *197*, 321–334.
(15) Burgess, J.; Frlec, B.; Holloway, J. H. *J. Chem. Soc., Dalton Trans.* **1974**, 1740–1742.
(16) Mallouk, T. E.; Rosenthal, G. L.; Muller, G.; Brusasco, R.; Bartlett, N. *Inorg. Chem.* **1984**, *23*, 3167–3173.
(17) Jenkins, H. D. B.; Roobottom, H. K.; Passmore, J.; Glasser, L. *Inorg. Chem.* **1999**, *38*, 3609–3620.
(18) Jenkins, H. D. B.; Tudela, D. *J. Chem. Educ.* **2003**, *80*, 1482–1487.
(19) Glasser, L.; Jenkins, H. D. B. *Chem. Soc. Rev.* **2005**, *34*, 866–874.
(20) Brownridge, S.; Calhoun, L.; Jenkins, H. D. B.; Laitinen, R. S.; Murchie, M. P.; Passmore, J.; Pietikäinen, J.; Rautiainen, J. M.; Sanders, J. C. P.; Schrobilgen, G. J.; Suontamo, R. J.; Tuononen, H. M.; Valkonen, J. U.; Wong, C.-M. *Inorg. Chem.* **2009**, *48*, 1938–1959.
(21) Gillespie, R. J.; Landa, B. *Inorg. Chem.* **1973**, *12*, 1383–1388.
(22) Gillespie, R. J.; Martin, D.; Schrobilgen, G. J. *J. Chem. Soc., Dalton Trans.* **1980**, 1898–1903.
(23) Edwards, A. J.; Holloway, J. H.; Peacock, R. D. *Proc. Chem. Soc.* **1963**, 275.
(24) Dean, P. A. W.; Gillespie, R. J.; Hulme, R.; Humphreys, D. A. *J. Chem. Soc.* (*A*) **1971**, 341–346.

Table 1. Summary of Crystal Data and Refinement Results for XeF_2, [XeF][MF_6] (M = As, Sb, Bi), [XeF][M_2F_{11}] (M = Sb, Bi), and [XeF_3][Sb_2F_{11}]

	XeF_2	XeF_2[a]	[XeF] [AsF_6]	[XeF] [AsF_6][b]	[XeF] [SbF_6]	[XeF] [BiF_6]
space group	*I*4/*mmm*	*I*4/*mmm*	$P2_1/n$	$P2_1/n$	$P2_1/c$	$P2_1/c$
a (Å)	4.2188(7)	4.315(3)	6.211(1)	6.308(3)	5.356(3)	5.235(2)
b (Å)	4.2188(7)	4.315(3)	6.169(1)	6.275(3)	10.898(5)	9.946(4)
c (Å)	6.991(2)	6.990(4)	15.793(3)	16.023(5)	10.926(5)	12.333(6)
β (deg)	90	90	100.03(3)	99.97(5)	94.055(7)	91.251(6)
V (Å^3)	124.43(5)	130.1(1)	595.8(2)	624.6(5)	636.20(5)	642.01(5)
Z	2	2	4	4	4	4
mol wt (g mol^{-1})	169.29	169.29	329.20	329.20	376.03	463.26
ρ_{calcd} (g cm^{-3})	4.519	4.32	3.782	3.61	4.030	4.896
T (°C)	−173	ambient	−173	24	−173	−173
μ (mm^{-1})	13.57		11.36	10.34	9.63	32.71
R_1[d]	0.0160	0.097	0.0269	0.033	0.0169	0.0409
wR_2[e]	0.0354		0.0646		0.0365	0.1076

	[XeF] [Sb_2F_{11}]	[XeF] [Sb_2F_{11}][c]	[XeF] [Bi_2F_{11}]	[XeF_3] [Sb_2F_{11}]	[XeF_3] [Sb_2F_{11}]
space group	$P2_1$	$P2_1$	$P2_12_12_1$	$P\bar{1}$ (2)	$P\bar{1}$ (2)
a (Å)	7.225(2)	7.33(1)	7.862(1)	7.929(3)	8.237(5)
b (Å)	9.392(3)	9.55(1)	9.568(1)	8.146(3)	9.984(20)
c (Å)	8.070(2)	8.07(1)	13.890(2)	9.493(3)	8.004(5)
α (deg)	90	90	90	67.676(9)	72.54(5)
β (deg)	106.734(5)	105.8(1)	90	88.38(2)	112.59(7)
γ (deg)	90	90	90	66.541(8)	117.05(21)
V (Å^3)	524.3(3)	543	1044.8(2)	514.8(3)	535(1)
Z	2	2	4	2	2
mol wt (g mol^{-1})	602.77	602.77	777.23	640.77	640.77
ρ_{calcd} (g cm^{-3})	3.818	3.69	4.941	4.134	3.98
T (°C)	−173	ambient	−173	−173	ambient
μ (mm^{-1})	8.47		36.97	8.66	
R_1[d]	0.0219	0.104	0.0395	0.0272	0.035
wR_2[e]	0.0491		0.0759	0.0694	0.03

[a] From refs 28, 30. [b] From ref 8. [c] From refs 9, 10. [d] $R_1 = \sum||F_o| - |F_c||/\sum|F_o|$ for $I > 2\sigma(I)$. [e] wR_2 is defined as $\{\sum[w(F_o^2 - F_c^2)^2]/\sum w(F_o^2)^2\}^{1/2}$ for $I > 2\sigma(I)$.

and conductometric[24,25] studies have shown that $As_2F_{11}^-$ is the dominant anionic species in HF solution at about −83 °C, failure to observe $As_2F_{11}^-$ as a discrete anion in HF solution by low-temperature ^{19}F NMR spectroscopy[24] implied that the anion was in equilibrium with AsF_5 and AsF_6^- and underwent rapid ^{19}F exchange (eq 2). Moreover, equilibrium 2 shifts

$$As_2F_{11}^- \rightleftharpoons AsF_5 + AsF_6^- \quad (2)$$

to the right at higher temperatures. Thus, attempts to crystallize [XeF][As_2F_{11}] by cooling HF solutions of XeF_2 and AsF_5 are likely to be unsuccessful owing to early crystallization of [XeF][AsF_6]. As in the case of [XeF][BiF_6] (vide supra), the greater lattice energy calculated for [XeF][AsF_6] (558 kJ mol^{-1}) relative to [XeF][As_2F_{11}] (480 kJ mol^{-1}) (Table 6) likely contributes to the lower solubility of [XeF][AsF_6] and its preferential crystallization. The As---F_b'---As bridge would be expected to be even more asymmetric in [XeF][As_2F_{11}] than in its bismuth analogue (see X-ray Crystallography), and the elongation of the second As---F_b' bond proximate to the Xe---F_b---As bridge could be sufficient to destabilize the $As_2F_{11}^-$ anion in favor of the [XeF][AsF_6] salt. In view of the lower fluoride ion donor strength of KrF_2 relative to that of XeF_2[26] (also see Computational Results), [KrF][As_2F_{11}] also is not expected to be stable. In view of these findings, a preliminary Raman spectroscopic study reporting evidence for the formation of [KrF][As_2F_{11}][27] should be re-examined.

Low-Temperature X-ray Crystal Structures of XeF_2, [XeF][MF_6] (M = As, Sb, Bi), [XeF][M_2F_{11}] (M = Sb, Bi), and [XeF_3][Sb_2F_{11}]. The single-crystal X-ray structures of XeF_2, [XeF][MF_6] (M = As, Sb, Bi), and [XeF][M_2F_{11}] (M = Sb, Bi) were determined at −173 °C. The unit cell parameters and refinement statistics for these salts are given in Table 1 where they are compared with those previously reported for XeF_2,[28−30] [XeF][RuF_6],[7] [XeF][AsF_6],[8] and [XeF][Sb_2F_{11}].[9,10] The geometrical parameters for [XeF][MF_6] (M = As, Sb, Bi), [XeF][M_2F_{11}] (M = Sb, Bi), and [XeF_3][Sb_2F_{11}] are provided in Tables 2 and 3. The synthesis and crystal structure of [XeF_3][Sb_2F_{11}] are described and discussed in the Supporting Information.

(a) XeF_2. The neutron diffraction[28] and single-crystal X-ray[29,30] structures of XeF_2 have been previously determined. The unit cell determined for XeF_2 in the previous X-ray study was tetragonal (*I*4/*mmm*; Table 1); however, the uncertainty in the Xe−F bond length (2.14(14) Å) was high because of the strong absorption that resulted from the use of Cu Kα X-rays. The neutron diffraction results were in agreement with the original study, and provided a significant improvement in the precision of the Xe−F bond length (2.00(1) Å).

(25) Barraclough, C. G.; Besida, J.; Davies, P. G.; O'Donnell, T. A. *J. Fluorine Chem.* **1988**, *38*, 405–419.
(26) Brock, D. S.; Casalis de Pury, J. J.; Mercier, H. P. A.; Schrobilgen, G. J.; Silvi, B. *Inorg. Chem.* **2010**, *49*, 6673–6689.
(27) Al-Mukhtar, M.; Holloway, J. H.; Hope, E. G.; Schrobilgen, G. J. *J. Chem. Soc., Dalton Trans.* **1991**, 2831–2834.
(28) Levy, H. A.; Agron, P. A. *J. Am. Chem. Soc.* **1963**, *85*, 241–242.
(29) Agron, P. A.; Begun, G. M.; Levy, H. A.; Mason, A. A.; Jones, C. G.; Smith, D. F. *Science* **1963**, *139*, 842–844.
(30) Siegel, S.; Gebert, E. *Chem. Commun.* **1963**, *85*, 240.

Table 2. Experimental and Calculated Geometrical Parameters of [XeF][AsF_6], [XeF][SbF_6], and [XeF][BiF_6]

	[XeF][AsF_6]				[XeF][SbF_6]			[XeF][BiF_6]		
			calcd			calcd			calcd	
	exptl	exptl [a]	PBE1PBE	MP2	exptl	PBE1PBE	MP2	exptl	PBE1PBE	MP2
					Bond Lengths (Å)					
Xe−F(1)	1.888(3)	1.873(6)	1.936	1.969	1.885(2)	1.927	1.964	1.913(7)	1.934	1.971
Xe---F(2)	2.208(3)	2.212(5)	2.089	2.131	2.278(2)	2.117	2.149	2.204(7)	2.094	2.127
M−F(2)	1.838(3)	1.813(6)	2.073	2.017	1.971(2)	2.131	2.127	2.108(7)	2.274	2.266
M−F(3)	1.683(4)	1.657(6)	1.680	1.709	1.857(2)	1.856	1.882	1.978(7)	1.959	1.985
M−F(5)	1.698(3)	1.683(8)	1.698	1.725	1.866(2)	1.865	1.890	1.953(7)	1.963	1.989
M−F(6)	1.687(3)	1.676(5)	1.698	1.725	1.868(2)	1.865	1.890	1.962(7)	1.963	1.989
M−F(4)	1.704(3)	1.690(5)	1.716	1.742	1.863(2)	1.883	1.910	1.954(7)	1.980	2.007
M−F(7)	1.709(3)	1.690(8)	1.716	1.742	1.860(2)	1.883	1.910	1.955(6)	1.980	2.007
					Bond Angles (deg)					
F(1)−Xe---F(2)	179.1(2)	178.9(7)	177.6	177.0	177.94(9)	177.5	177.0	178.4(3)	177.9	177.5
Xe---F(2)−M	133.6(2)	134.8(2)	122.5	119.2	136.9(1)	122.3	119.3	156.1(4)	123.0	119.6
					Dihedral Angle (deg)					
Xe---F(2)−M−F(4)	44.2		44.5	44.3	18.8	44.2	44.0	8.6	44.1	44.1

[a] From ref 8.

Table 3. Experimental Geometrical Parameters of [XeF][Sb_2F_{11}], [XeF][Sb_2F_{11}], and [XeF_3][Sb_2F_{11}]

	[XeF][Sb_2F_{11}]	[XeF][Sb_2F_{11}][a]	[XeF][Bi_2F_{11}]		[XeF_3][Sb_2F_{11}]	[XeF_3][Sb_2F_{11}][b]
			Bond Lengths (Å)			
Xe−F(1)	1.888(4)	1.82(3)	1.909(6)	Xe−F(1)	1.908(4)	1.89(1)
Xe−F(2)	2.343(4)	2.34(3)	2.253(5)	Xe−F(2)	1.832(4)	1.83(1)
M−F(2)	1.930(3)	1.91(3)	2.075(6)	Xe−F(3)	1.883(4)	1.88(1)
M−F(3)	1.855(3)	1.84(4)	1.937(6)	Xe−F(4)	2.490(4)	2.50(1)
M−F(4)	1.844(3)	1.86(4)	1.930(6)	Sb(1)−F(4)	1.901(4)	1.90(1)
M−F(5)	1.848(3)	1.81(4)	1.955(5)	Sb(1)−F(5)	1.840(4)	1.84(1)
M−F(6)	1.856(3)	1.80(4)	1.950(6)	Sb(1)−F(6)	1.844(4)	1.83(1)
M−F(7)	2.010(3)	1.93(3)	2.092(6)	Sb(1)−F(7)	1.849(4)	1.85(1)
Sb(2)−F(7)	2.066(3)	2.10(3)	2.195(6)	Sb(1)−F(8)	1.860(4)	1.85(1)
Sb(2)−F(8)	1.851(4)	1.96(5)	1.956(6)	Sb(1)−F(9)	2.018(4)	2.01(1)
Sb(2)−F(9)	1.859(3)	1.75(6)	1.959(5)	Sb(2)−F(9)	2.034(4)	2.04(1)
Sb(2)−F(10)	1.857(3)	1.76(6)	1.958(6)	Sb(2)−F(10)	1.853(4)	1.85(1)
Sb(2)−F(11)	1.862(4)	1.74(6)	1.970(6)	Sb(2)−F(11)	1.848(4)	1.84(1)
Sb(2)−F(12)	1.864(3)	1.88(5)	1.954(6)	Sb(2)−F(12)	1.850(4)	1.86(1)
				Sb(2)−F(13)	1.878(4)	1.86(1)
				Sb(2)−F(14)	1.861(4)	1.86(1)
			Bond Angles (deg)			
F(1)−Xe−F(2)	179.3(2)	176(1)	178.9(3)	F(1)−Xe−F(2)	80.3(2)	80.2(3)
Xe−F(2)−M	148.1(2)	149(2)	151.3(3)	F(1)−Xe−F(3)	161.3(2)	161.9(4)
Sb−F(7)−Sb(2)	146.0(2)	149(2)	145.3(3)	F(1)−Xe−F(4)	125.0(2)	125.3(3)
				F(2)−Xe−F(3)	81.2(2)	81.7(3)
				F(2)−Xe−F(4)	154.5(2)	154.4(4)
				F(3)−Xe−F(4)	73.4(2)	72.7(3)
				Xe−F(4)−Sb	169.0(2)	171.6(1)
				Sb−F(9)−Sb(2)	155.0(2)	155.4(2)
			Dihedral Angle (deg)			
Xe−F(2)−M−F(4)	7.9		5.5			

[a] From ref 10. [b] From ref 45.

In light of the present study of XeF^+ salts and the fundamental importance of XeF_2 as an anchor point for comparisons of the Xe−F bond length data, the crystal structure of XeF_2 has been redetermined (Supporting Information, Figure S1) to obtain a more precise Xe−F bond length. Xenon difluoride retains *I*4/*mmm* crystallographic symmetry at −173 °C; however, a modest contraction of the unit cell occurs along the *a*- and *b*-axes, whereas the *c*-axis remains unaffected (Table 1). The more precise Xe−F bond length determined at −173 °C (1.999(4) Å) is in agreement with the earlier crystallographic studies, and shows that the Xe−F bond lengths are significantly longer in the solid state than in the gas phase (Raman, 1.9791(1);[31] infrared,1.974365(7)[32]). The elongation is attributed to the eight intermolecular Xe···F contacts (3.338 Å), which lie within the sum of

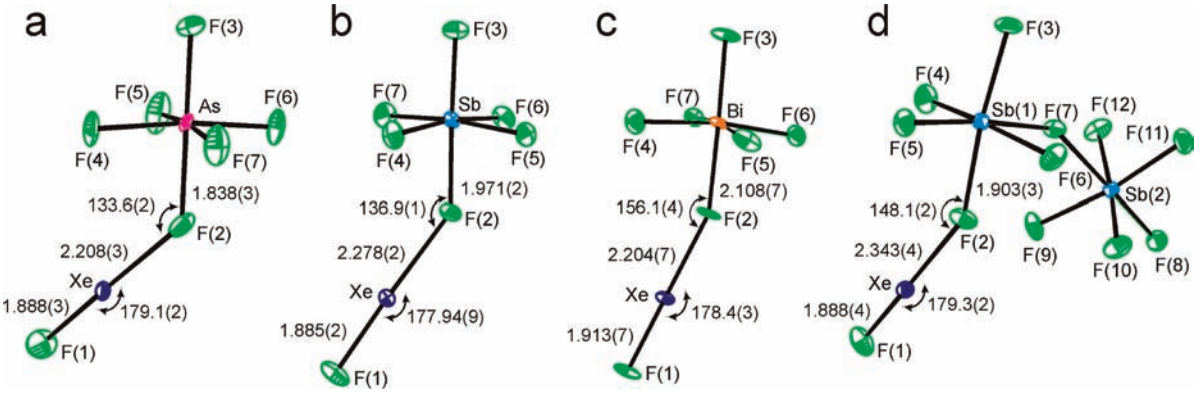

Figure 1. Crystal structures of the (a) $[XeF][AsF_6]$, (b) $[XeF][SbF_6]$, (c) $[XeF][BiF_6]$, and (d) $[XeF][Sb_2F_{11}]$ salts with thermal ellipsoids drawn at the 50% probability level.

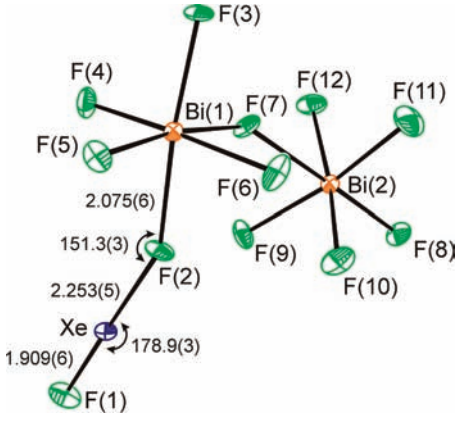

Figure 2. Crystal structure of the $[XeF][Bi_2F_{11}]$ salt with thermal ellipsoids drawn at the 50% probability level.

the xenon (2.16 Å) and fluorine (1.47 Å) van der Waals radii[33] and serve to give the xenon and fluorine centers high secondary sphere coordination numbers that lower the atomic charge of xenon and increase the ionic characters of the Xe−F bonds (Figure S1, Supporting Information).

(b) $[XeF][AsF_6]$, $[XeF][SbF_6]$, $[XeF][BiF_6]$, $[XeF][Sb_2F_{11}]$, and $[XeF][Bi_2F_{11}]$. The bond lengths, bond angles, and contact distances determined for $[XeF][MF_6]$ (M = As, Sb, Bi), and $[XeF][M_2F_{11}]$ (M = Sb, Bi) are summarized in Tables 2 and 3, respectively. The XeF^+ cations in $[XeF][MF_6]$ (M = As, Sb, Bi) and $[XeF][M_2F_{11}]$ (M = Sb, Bi) are strongly coordinated to the MF_6^- and $M_2F_{11}^-$ anions through single fluorine bridges (Figures 1 and 2).

(i) Xe−F_t, Xe---F_b, and M---F_b Bond Lengths. The Xe−F_t (F_t, terminal fluorine) bond lengths in $[XeF][AsF_6]$ (1.888(3) Å), $[XeF][SbF_6]$ (1.885(2) Å) and $[XeF][Sb_2F_{11}]$ (1.888(4) Å) are not significantly different within $\pm 3\sigma$, but are shorter than those of $[XeF][BiF_6]$ (1.913(7) Å) and $[XeF][Bi_2F_{11}]$ (1.909(6) Å). The Xe−F_t bond lengths determined from the X-ray crystal structures of $[XeF][MF_6]$ and $[XeF][M_2F_{11}]$ are shorter than those of crystalline (vide supra) and gaseous XeF_2.[31,32] The same trend is observed for the Kr−F_t bond lengths (1.765(3) × 2, 1.774(6), 1.783(6) Å) of the $[KrF][MF_6]$ (M = As, Sb, Bi, Au) salts and the Kr−F bond length (1.894(5) Å) of α-KrF_2.[1] This trend is consistent with 3 center−4 electron molecular orbital (MO) descriptions of NgF_2[34] and valence bond Structures I and II which predict formal Ng−F bond orders of one-half for NgF_2 and one for the free NgF^+ cations.

$$F^- \ {}^+Ng-F \leftrightarrow F-Ng^+ \ F^-$$
$$\text{I} \qquad\qquad \text{II}$$

The Xe---F_b and M---F_b (F_b, bridging fluorine) bond lengths of the XeF^+ salts investigated in the present study are elongated with respect to those of XeF_2 and the non-bridging M−F bond lengths of their counteranions. The Xe---F_b bond lengths differ little among the $[XeF][AsF_6]$ (2.208(3) Å), $[XeF][BiF_6]$ (2.204(7) Å), and $[XeF][RuF_6]$ (2.182(15) Å)[7] salts, but is significantly longer in $[XeF][SbF_6]$ (2.278(2) Å).

The M---F_b bond lengths of $[XeF][AsF_6]$ (1.838(3) Å), $[XeF][SbF_6]$ (1.971(2) Å), $[XeF][BiF_6]$ (2.108(7) Å), $[XeF][Sb_2F_{11}]$ (1.930(3) Å), and $[XeF][Bi_2F_{11}]$ (2.075(6) Å) are longer than the average terminal M−F bond lengths of the anions, which are 1.697(7), 1.863(4), 1.960(15), 1.855(10), and 1.952(17) Å, respectively. Although elongation of the M---F_b (M−F(2)) bond might be expected to lead to shortening of the M−F(3) bond with increasing strength of the parent Lewis acid as a result of the *trans*-influence, the M−F(3) bond lengths do not differ significantly from the remaining non-bridging bond lengths of the anions in $[XeF][MF_6]$ (M = As, Sb, Bi) and $[XeF][M_2F_{11}]$ (M = Sb, Bi).

(ii) F−Xe---F_b and Xe---F_b---M Bond Angles. The Ng---F_b---M angles in both the XeF^+ and the KrF^{+1} salts are bent and are consistent with $AXYE_2$ VSEPR arrangements at their respective fluorine bridge atoms, which, because of the high ionic characters of these bonds, are significantly more open than the ideal tetrahedral angle. The F_t−Ng---F_b angles are highly deformable, and are likely influenced by crystal packing. The deformability of the Xe---F_b---M angles in the present series of salts is supported by the low in-plane Xe---F_b---M bending frequencies calculated for the $[XeF][AsF_6]$ (57 cm^{-1}), $[XeF][SbF_6]$ (55 cm^{-1}), and $[XeF][BiF_6]$ (46 cm^{-1}) ion pairs (see Vibrational Frequencies). The Ng---F_b---M

(31) Brassington, N. J.; Edwards, H. G. M.; Long, D. A. *J. Chem. Soc., Faraday Trans. 2* **1978**, *74*, 1208–1213.
(32) Bürger, H.; Kuna, R.; Ma, S.; Breidung, J.; Thiel, W. *J. Chem. Phys.* **1994**, *101*, 1–14.
(33) Bondi, A. *J. Phys. Chem.* **1964**, *68*, 441–451.
(34) Rundle, R. E. *J. Am. Chem. Soc.* **1963**, *85*, 112–113.

angles are similar in $[XeF][AsF_6]$ (133.6(2)°), $[XeF][SbF_6]$ (136.9(1)°), $[XeF][RuF_6]$ (137.2(5)°), $[KrF][AsF_6]$ (133.7(3)°), $[KrF][SbF_6]$ (139.2(2)°), $[KrF][BiF_6]$ (138.3(3)°), and $[KrF][AuF_6]$ (125.3(7)°) but this angle is much larger in $[XeF][BiF_6]$ (156.1(4)°). In view of the smaller but similar Xe/Kr---F_b---M bond angles calculated for the $[NgF][AsF_6]$ (122.5/119.6°), $[NgF][SbF_6]$ (126.0/119.4°), and $[NgF][BiF_6]$ (126.5/119.8°) ion pairs (see Computational Results), and the similar bond angles determined in the structures of $[XeF][Sb_2F_{11}]$ (146.0(2)°) and $[XeF][Bi_2F_{11}]$ (145.3(3)°), the larger Xe---F_b---M bond angle of $[XeF][BiF_6]$ is likely a consequence of crystal packing which results in the near-eclipsed Xe---F_b---Bi−F(4) arrangement which is unique among the series of $[NgF][MF_6]$ salts (vide infra) investigated thus far. The long Xe···F contacts lying within the sum of the van der Waals radii of xenon (2.16 Å) and fluorine (1.47 Å)[33] are presumed to be the main cause of the overall larger Xe---F_b---M bond angles in the solid state (Tables 2 and 3). These contacts are most numerous for $[XeF][AsF_6]$, where twelve Xe···F interactions ranging from 3.164 to 3.491 Å were identified. The structures of $[XeF][SbF_6]$, $[XeF][BiF_6]$, and $[XeF][Sb_2F_{11}]$ each have nine Xe···F contacts with distances ranging from 3.118 to 3.581 Å, 3.110 to 3.513 Å, and 3.115 to 3.592 Å, respectively. The crystal structure of $[XeF][Bi_2F_{11}]$ exhibits seven Xe···F contacts, with distances ranging from 3.064 to 3.439 Å.

The F−Xe---F_b bond angle is slightly bent, within $\pm 3\sigma$, in the structures of $[XeF][SbF_6]$ (177.94(9)°), $[XeF][AsF_6]$ (179.1(2)°), $[XeF][BiF_6]$ (178.4(3)°), $[XeF][Sb_2F_{11}]$ (179.3(2)°), and $[XeF][Bi_2F_{11}]$ (178.9(3)°). Similar F−Kr---F_b angles have been noted for the $[KrF][MF_6]$ salts[1] and it has been suggested that they arise from the repulsive interactions between the valence electron lone pairs of F_b and Kr. These angles are reproduced in the calculated structures of the $[NgF][MF_6]$ (Ng = Kr, Xe; M = As, Sb, Bi) salts (see Computational Results).

The conformational extremes of the F_t−Xe---F_b---M moiety with respect to the equatorial fluorine atoms of the anion range from the eclipsed conformation (Structure III), which maximizes the steric interaction between the XeF^+ cation and the next nearest fluorine atom (F''_e), to the staggered conformation (Structure IV), which minimizes the steric interactions between the cation and the fluorine ligands of the anion. The angle between the [F(4), M, F(2)]-plane and the [M, F(2), Xe]-plane,

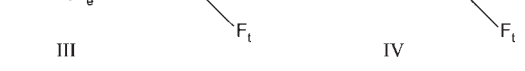

that is, the Xe---F(2)---M−F(4) dihedral angle, ranges from 44.2° (As, near-staggered conformation) to 18.8° (Sb, gauche conformation) to 8.6° (Bi, gauche/near-eclipsed conformation). The large variations in the Xe---F(2)---M−F(4) dihedral angles imply that the energy differences between the conformational extremes are small, in accordance with the low frequencies calculated for the F_t−Xe---F_b---M torsional motions of these species (see Vibrational Frequencies), and that these dihedral angles are susceptible to crystal packing.

(iii) $Sb_2F_{11}^-$ and $Bi_2F_{11}^-$. The X-ray crystal structures of $As_2F_{11}^-$ and $Sb_2F_{11}^-$ have been previously determined for a number of salts, but the $Bi_2F_{11}^-$ anion had only been characterized by Raman spectroscopy for $[XeF][Bi_2F_{11}]$, $[XeF_3][Bi_2F_{11}]$, and $[Cs][Bi_2F_{11}]$.[22] The structure of $[XeF][Bi_2F_{11}]$ provides the first crystallographic characterization of the $Bi_2F_{11}^-$ anion. Like its lighter analogues, the $Bi_2F_{11}^-$ anion is composed of two pseudo-octahedrally coordinated pnictogen atoms bridged by a fluorine atom (F_b') (Figure 2). The Bi---F_b'---Bi bond angle (145.3(3)°) is similar to the Sb---F_b'---Sb (146.0(2)°) bond angle in $[XeF][Sb_2F_{11}]$. Although $[XeF][As_2F_{11}]$ remains unknown, similar bond angles have been reported for $As_2F_{11}^-$ in $[(m\text{-}CF_3C_6H_4)(C_6H_5)CF][As_2F_{11}]$ (156.5(13)°),[35] $[(CH_3S)_2CSH][As_2F_{11}]$ (159.1(6)°),[36] $[Cl_3PH][As_2F_{11}]$ (148.3(2)°),[37] and $[Br_3PH][As_2F_{11}]$ (145.9(4)°).[37]

Prior quantum-chemical calculations of the free $Sb_2F_{11}^-$ anion constrained the symmetry to D_{4h} with an Sb---F_b'---Sb angle of 180° and an eclipsed conformation for the two SbF_4 planes.[38] In a more recent study,[39] the use of C_1 as a starting symmetry allowed the Sb---F_b'---Sb angle to bend and the SbF_4 planes to rotate, achieving an Sb---F_b'---Sb angle of 133.7° and a dihedral angle of 37.7° for the staggered conformational relationship between the SbF_4 planes. Both structural changes led to better agreement between the observed and calculated bond lengths, angles, and vibrational frequencies.

Edwards and co-workers have investigated the effects of close-packing arrangements of the light atoms for the polymeric fluorine-bridged species $TcOF_4$,[40] $MoOF_4$,[41] WOF_4,[42] and $ReOF_4$.[43] These studies demonstrated that the ideal bridge angle is 132° if the central metal atoms lie within the octahedral interstitial sites of hexagonal close-packed oxygen and fluorine atoms, but is 180° if the metal atoms lie within the octahedral sites of a cubic close-packed lattice of oxygen and fluorine atoms. The packing of the fluorine atoms in the structures of $[XeF][Sb_2F_{11}]$, $[XeF_3][Sb_2F_{11}]$, and $[XeF][Bi_2F_{11}]$ most closely resemble hexagonal close-packed arrangements and is consistent with their bent anion geometries in the solid state. The larger Sb(1)---F(7)---Sb(2) angles in the crystal structures of $[XeF][Sb_2F_{11}]$ (146.0(2)°) and $[XeF_3][Sb_2F_{11}]$ (155.0(2)°) compared to the calculated value for the gas-phase anion are likely consequences of hexagonal close packing of the fluorine atoms. Moreover, the low frequency calculated for the Sb---F_b'---Sb bend of the gas-phase $Sb_2F_{11}^-$ anion (23 cm^{-1})[39] underscores the deformability of this angle, and its susceptibility to crystal packing.

(35) Christe, K. O.; Zhang, X.; Bau, R.; Hegge, J.; Olah, G. A.; Prakash, G. K. S.; Sheehy, J. A. *J. Am. Chem. Soc.* **2000**, *122*, 481–487.
(36) Minkwitz, R.; Neikes, F. *Inorg. Chem.* **1999**, *38*, 5960–5963.
(37) Minkwitz, R.; Dzyk, M. *Eur. J. Inorg. Chem.* **2002**, 569–572.
(38) Sham, I. H. T.; Patrick, B. O.; von Ahsen, B.; von Ahsen, S.; Willner, H.; Thompson, R. C.; Aubke, F. *Solid State Sci.* **2002**, *4*, 1457–1463.
(39) Hughes, M.; Mercier, H. P. A.; Schrobilgen, G. J. *Inorg. Chem.* **2010**, *49*, 271–284.
(40) Edwards, A. J.; Jones, G. R.; Sills, R. J. C. *J. Chem. Soc.* (*A*) **1970**, 2521–2523.
(41) Edwards, A. J.; Steventon, B. R. *J. Chem. Soc.* (*A*) **1968**, 2503–2510.
(42) Edwards, A. J.; Jones, G. R. *J. Chem. Soc.* (*A*) **1968**, 2074–2078.
(43) Edwards, A. J.; Jones, G. R. *J. Chem. Soc.* (*A*) **1968**, 2511–2515.

The MF_4 groups of the $M_2F_{11}^-$ (M = Sb, Bi) anions are nearly staggered with dihedral angles, ψ, between the equatorial planes of each MF_5 unit of 40.6° [planes F(2,3,5,7) and F(7,8,9,11)] and 44.3° [planes F(4,5,6,7) and F(7,8,10,12)] for $Sb_2F_{11}^-$ and 38.8° [planes F(2,3,5,7) and F(7,8,9,11)] and 41.4° [planes F(4,5,6,7) and F(7,8,10,12)] for $Bi_2F_{11}^-$. A well documented correlation exists between the M---F_b'---M bridge angle of a $M_2F_{11}^-$ anion and ψ,[44] which has been associated with minimization of the steric repulsions between the nearest neighbor fluorine atoms of each octahedron as the M---F---M angle decreases and ψ increases. Accordingly, ψ is 0° when the M---F_b'---M angle is 180°, reaching a maximum of 45° when the M---F_b'---M is the smallest at about 145°. In the present cases, the ψ angles (38.8−44.3°) and bridge bond angles (Sb, 146.0(2)° and Bi, 145.3(3)°) are in accordance with this relationship.

Because the $M_2F_{11}^-$ anions are of lower symmetry than the MF_6^- anions, it is difficult to predict a preferred orientation for the F_t−Xe---F_b groups in the [XeF]-[M_2F_{11}] ion pairs, particularly when long Xe···F contacts within the crystal lattices are taken into account. The F_t−Xe---F_b groups are nearly eclipsed for [XeF][M_2F_{11}], with Xe---F_b---M−F(4) dihedral angles of 7.9 (Sb) and 5.5° (Bi).

The strengths of interactions between the $M_2F_{11}^-$ anions and the XeF^+ cations are reflected in the asymmetries of their M---F_b'---M bridge bond lengths, where the M---F_b' bond is shorter for the pnictogen that is fluorine bridged to the XeF^+ cation. The asymmetry of the M---F_b' bonds is less pronounced for the $Sb_2F_{11}^-$ salt (2.010(3), 2.066(3) Å) than it is for the $Bi_2F_{11}^-$ salt (2.092(6), 2.195(6) Å), consistent with a greater degree of ionic character for the former salt (see Xe−F Bond Length Correlations).

Unlike the octahedral MF_6^- anions where the six fluorines have equivalent fluorobasicities, the $M_2F_{11}^-$ anions have two axial positions and eight equivalent equatorial positions if F_b' of the M---F_b'--- M bridge is ignored. The M---F_b' bridge bonds of the $M_2F_{11}^-$ anions induce a *trans*-influence, so that the axial fluorine ligands are less fluoro-basic than the equatorial fluorine ligands, resulting in *cis*-fluorine bridged structures for the [XeF][M_2F_{11}] salts. Coordination of the cation to an equatorial fluorine position of the $M_2F_{11}^-$ anion is not unique to the XeF^+ salts, and is also observed for [XeF_3][Sb_2F_{11}][45] (also see Supporting Information) and [OsO_2F_3][Sb_2F_{11}].[39] An exception to this preference is [XeCl][Sb_2F_{11}], for which X-ray crystallography has shown that the xenon atom is bridged to an axial fluorine atom of the $Sb_2F_{11}^-$ anion.[46] This reflects the lower bond polarity and Lewis acidity of $XeCl^+$ relative to that of XeF^+, which arises as a consequence of the smaller electronegativity difference between chlorine and xenon that is also apparent from the significantly longer Xe---F_b bond lengths in [XeCl][Sb_2F_{11}] (2.612(4), 2.644(4) Å) relative to that of [XeF][Sb_2F_{11}] (2.278(2) Å).

(iv) Xe−F and M−F Bond Lengths and the Lewis Acidities of MF_5 and M_2F_{10}. In the gaseous state, the Xe−F bond lengths and vibrational frequencies of the fluorine-bridged [XeF][MF_6] and [XeF][M_2F_{11}] ion pairs are expected to vary depending on the fluoride ion acceptor strengths of the parent MF_5 and M_2F_{10} Lewis acids. Christe and Dixon[47,48] have provided a quantitative Lewis acidity scale based on the absolute fluoride ion affinity (FIA) of a Lewis acid, where the FIA is defined as the negative heat of formation for the gas-phase reaction between a Lewis acid and fluoride ion. The calculated FIAs of the pnictogen pentafluorides increase in the order, PF_5 (394.7 kJ mol^{-1}) < AsF_5 (443.1 kJ mol^{-1}) < BiF_5 (466.9 kJ mol^{-1}) < SbF_5 (495.0 kJ mol^{-1})[i] at the MP2/aug-cc-pVDZ level of theory.[48]

As previously observed for the [KrF][MF_6] (M = As, Sb, Bi) salts,[1] the Xe−F_t bond lengths in the present series of salts also showed no correlation with the FIAs of the parent MF_5 (M = As, Sb, Bi) or M_2F_{10} (M = Sb, Bi). With the exception of [XeF][BiF_6] and [XeF][Bi_2F_{11}], which exhibit slightly longer Xe−F_t bond lengths, this bond length is essentially invariant for [XeF][AsF_6], [XeF][SbF_6], and [XeF][Sb_2F_{11}].

Although the Xe---F_b bonds are, overall, more sensitive to the Lewis acidities of MF_5 and M_2F_{10} than the Xe−F_t bonds, the Xe---F_b bond lengths of [XeF][AsF_6] and [XeF][BiF_6] cannot be differentiated, with calculated FIAs for AsF_5 and BiF_5 that differ by 23.8 kJ mol^{-1}.[48] The Xe---F_b bond length of [XeF][SbF_6], which is significantly longer than those of [XeF][AsF_6] and [XeF]-[BiF_6], is in overall accord with the FIAs for AsF_5 and BiF_5 which are 51.9 and 28.1 kJ mol^{-1} lower, respectively, than that of SbF_5.[48]

The higher FIAs of Sb_2F_{10} (526.8 kJ mol^{-1}) and Bi_2F_{10} (510.0 kJ mol^{-1}) compared to those of MF_5[48] are a consequence of greater dispersal of the negative charge among the fluorine atoms of the $M_2F_{11}^-$ (M = Sb, Bi) anions. This trend is reflected in the relative Xe---F_b bond lengths of [XeF][Sb_2F_{11}] (2.343(4) Å) and [XeF][Bi_2F_{11}] (2.253(5) Å). It is noteworthy that the Xe---F_b bond length of [XeF][Bi_2F_{11}] is shorter than that of [XeF][SbF_6] despite the fact that Bi_2F_{10} is a stronger Lewis acid than SbF_5. The Xe---F_b bond lengths of the XeF^+ salts increase in the order $BiF_5 \approx AsF_5 < Bi_2F_{10} < SbF_5 < Sb_2F_{10}$, with a similar order observed for the Kr---F_b bond lengths of the [KrF][MF_6] salts, that is, $BiF_5 < AsF_5 \approx SbF_5$,[1] which are both at variance with the trends predicted on basis of FIAs alone.

The relative Lewis acidities of MF_5 (M = As, Sb, Bi) and M_2F_{10} (M = Sb, Bi) are reflected in the M---F_b bond lengths. Thus, the longer M---F_b bond lengths determined for the $Sb_2F_{11}^-$ and $Bi_2F_{11}^-$ salts relative to those of the SbF_6^- and BiF_6^- salts are consistent with greater degree of fluoride ion transfer in the $M_2F_{11}^-$ salts as a result of the higher Lewis acidities of Sb_2F_{10} and Bi_2F_{10}. The difference between the M---F_b bond length and the average non-bridging M−F bond lengths of the anion may also be correlated with the fluoride ion acceptor

(44) D.M. Bruce, D. M.; Holloway, J. H.; Russel, D. R. *J. Chem. Soc., Dalton. Trans.* **1978**, 1627–1631.
(45) McKee, D.; Zalkin, A.; Bartlett, N. *Inorg. Chem.* **1973**, *12*, 1713–1717.
(46) Seidel, S.; Seppelt, K. *Angew. Chem., Int. Ed.* **2001**, *40*, 4225–4227.
(47) Christe, K. O.; Dixon, D. A.; McLemore, D.; Wilson, W. W.; Sheehy, J. A.; Boatz, J. A. *J. Fluorine Chem.* **2000**, *101*, 151–153.
(48) Christe, K. O.; Dixon, D. A. Recent Progress on the Christe/Dixon Quantitative Scale of Lewis Acidity. Presented at the 92nd Canadian Society for Chemistry Conference, Hamilton, ON, May−June 2009.

Table 4. Experimental and Calculated Vibrational Frequencies (cm^{-1}) for [XeF][AsF_6], [XeF][SbF_6], and [XeF][BiF_6]

[XeF][AsF_6]		[XeF][SbF_6]		[XeF][BiF_6]		
exptl[a,b]	calcd[c]	exptl[a,d]	calcd[c]	exptl[a,e]	calcd[c]	assgnts (C_s)[f]
731(7)	766(2)[131] [g]	677(5) 672(41)	695(9)[93]		618(16)[56] [h]	$\nu(MF_7)$
				590(12)		
724(10)	763(6)[152] [i]	688(2) 682(11)	700(2)[124]		612(13)[71]	$[\nu(MF_3)+\nu(MF_4)]-[\nu(MF_5)+\nu(MF_6)]$
	763(1)[154]		698(<1)[125]		611(1)[91]	$[\nu(MF_3)+\nu(MF_5)]-[\nu(MF_4)+\nu(MF_6)]$
680(39)	690(17)[26]	647(26)	647(20)[30]	588(100)	583(29)[17]	$[\nu(MF_3)+\nu(MF_4)+\nu(MF_5)+\nu(MF_6)]$
589(1)	611(2)[2]	588(8)	596(2)[3]	545(4) 541(9)	550(4)[4]	$[\nu(MF_4)+\nu(MF_5)]-[\nu(MF_3)+\nu(MF_6)]$
611(100) 607(96)	600(39)[125]	621(66) 616(100)	609(41)[111]	608(11) 602(48)	601(37)[162] [j]	$\nu(XeF_1)$
464(4)	476(14)[115]	485(6) 473(10)	441(10)[201]	439(<1) 417(<1)	441(13)[222]	$\nu(XeF_2)-\nu(MF_2)$
420(7)	395(<1)[11]	290(8) 282(3)	289(1)[6]	242(5)	235(2)[2]	$[\delta(F_3MF_4)+\delta(F_5MF_6)]$
	389(<1)[33] [k]	272(6)	270(<1)[54]	219(<1)	209(<1)[34]	$\delta(MF_5F_6F_7)-\delta(F_3MF_4)$
378(4)	383(<1)[48]		278(<0.1)[50]	207(3) 203(1)	206(<1)[62]	$[\delta(F_3MF_5)-\delta(F_4MF_6)]+\delta(F_2MF_7)_{oop}$
344(32)	366(<1)[21] [l]	340(2), br	353(1)[24]		313(<1)[34]	$[\nu(XeF_2)+\nu(MF_2)]$
	312(<1)[<1]	264(4)	253(<1)[2]	228(4)	232(<1)[2]	$\rho_t(F_2MF_7)_{oop}+\rho_t(F_4MF_5)_{oop}-\rho_t(F_3MF_6)_{oop}$
276(1)	288(2)[102] [m]	211(2)	212(1)[5]	194(<1)	169(2)[5]	$\delta(MF_5F_6F_7)$
242(<1)	276(<0.1)[188] [n]	268(3)	263(<1)[155]	186(<1)	206(<1)[68]	$\delta(MF_3F_4F_7)$
223(<1)	234(<0.1)[3]		193(<1)[2]	175(<1)	167(<1)[2]	$[\delta(F_3MF_5)-\delta(F_4MF_6)]+\rho_t(F_2AsF_7)$
	181(<0.1)[<1]	153(6)	143(<1)[<1]	123(1)	117(<1)[<1] [o]	$[\rho_w(F_3MF_6)-\rho_w(F_4MF_5)]$
164(7) 160(7)	151(<1)[3]	136(7)	126(<1)[<1]		93(<0.1)[<0.1]	$[\delta(F_2MF_7)_{oop}-\rho_t(F_2XeF_1)]+[\rho_w(F_3MF_6)-\rho_w(F_4MF_5)]_{small}$
149(6) 143(6)	146(<1)[4]		119(<1)[2]		94(<1)[<1]	$\rho_r(MF_3F_4F_5F_6F_7)$
120(<1), br	135(1)[9]	147(6)	147(1)[2]	138(3)	141(1)[2]	$\delta(F_1XeF_2)_{ip}$
	57(<1)[<1]		55(<1)[<1]		46(<1)[<1]	$\delta(MF_2Xe)_{ip}$
	28(<1)[<0.1]		27(<1)[<0.1]		22(<1)[<0.1]	XeF_t torsion about $M-F_2+(MF_5)_{rock}$
				82(3) 76(2) 72(2)		lattice modes

[a] The experimental Raman intensities (in parentheses) are relative intensities with the most intense band given a value of 100. [b] Present work. [c] PBE1PBE/aug-cc-pVQZ(-PP). Values in parentheses denote calculated Raman intensities ($Å^4$ u^{-1}) and values in square brackets denote calculated infrared intensities (km mol^{-1}). [d] Present work. [e] Experimental values are taken from ref 22. Bands observed at 82(3), 76(2), 72(2), 62(6), 53(3), 44(2) cm^{-1} were originally assigned to external modes. [f] The abbreviations oop and ip denote out of plane and in plane, respectively. The plane contains $F_1XeF_2AsF_7$. [g] The description should read: $\nu(AsF_7)-[\nu(AsF_5)+\nu(AsF_6)]+[\nu(AsF_3)+\nu(AsF_4)]_{small}$. [h] The description should read: $\nu(BiF_7)+\nu(XeF_1)_{small}$. [i] The description should read: $[\nu(AsF_3)+\nu(AsF_4)]-[\nu(AsF_5)+\nu(AsF_6)]-\nu(AsF_7)$. [j] The description should read: $\nu(XeF_1)-\nu(BiF_7)_{small}$. [k] The description should read: $\delta(AsF_5F_6F_7)-\delta(F_3AsF_4)+\nu(AsF_2)$. [l] The description should read: $[\nu(XeF_2)+\nu(AsF_2)]+\delta(AsF_3F_4F_7)$. [m] The description should read: $\delta(AsF_5F_6F_7)+\nu(AsF_2)$. [n] The description should read: $\delta(AsF_3F_4F_7)+\nu(AsF_2)$. [o] The description should read: $[\rho_w(F_3MF_6)-\rho_w(F_4MF_5)]+\rho_w(F_2BiF_7)$.

strength. Anions derived from the strongest Lewis acids exhibit the smallest difference between the M---F_b and M−F bond lengths because of the greater degree of fluoride ion transfer and a weaker cation−anion interaction. The differences between the M---F_b and the average non-bridging M−F bond lengths are greater for [XeF][AsF_6] (0.14 ± 0.01 Å) and [XeF][BiF_6] (0.15 ± 0.02 Å) when compared with that of [XeF][SbF_6] (0.108 ± 0.006 Å), and greater for [XeF][Bi_2F_{11}] (0.15 ± 0.01 Å) when compared with that of [XeF][Sb_2F_{11}] (0.08 ± 0.01 Å). These trends are consistent with the relative fluoride ion acceptor properties of the parent Lewis acids arrived at by comparisons of the Xe---F_b bond lengths (vide supra).

In addition to variations in the Xe---F_b and M---F_b bond lengths, the relative Lewis acidities of M_2F_{10} may be related to the degree of asymmetry in the M---F_b'---M bridging bond lengths. In the case of a strong fluoride ion acceptor, the interaction between the cation and the anion will be minimized, resulting in a highly symmetric $M_2F_{11}^-$ anion. For weaker Lewis acids, the cation−anion interaction becomes more significant and is expected to contract the M---F_b' bond closest to the site of coordination while lengthening the remaining M---F_b' bond. The M---F_b' bonds in [XeF][Sb_2F_{11}] (2.010(3), 2.066(3) Å) and [XeF][Bi_2F_{11}] (2.092(6), 2.195(6) Å) clearly exhibit this trend with a greater degree of asymmetry being observed in the $Bi_2F_{11}^-$ salt. This trend is in accord with the lower FIA calculated for Bi_2F_{10} (510.0 kJ mol^{-1}) compared with that of Sb_2F_{10} (526.8 kJ mol^{-1}). Although the FIA of As_2F_{10} has not been reported, the value for BiF_5 (466.9 kJ mol^{-1}) exceeds that of AsF_5 (443.1 kJ mol^{-1}), suggesting that the FIA of As_2F_{10} should be less than that of Bi_2F_{10}. Therefore, the M---F_b'---M bridge would be expected to be even more asymmetric in [XeF][As_2F_{11}] than in [XeF][Bi_2F_{11}], and the elongation of the M---F_b' bond proximate to the Xe---F_b---As bridge will tend to destabilize the $As_2F_{11}^-$ anion in favor of the [XeF][AsF_6] salt (see section on Thermochemistry of Noble-Gas Fluorocation Salts). This factor and the lower lattice energy of [XeF][As_2F_{11}] (480 kJ mol^{-1}) relative to that of [XeF][AsF_6] (546 kJ mol^{-1}) (see Table 6) may account for the inability to prepare [XeF][As_2F_{11}] by the direct reaction of XeF_2 and [XeF][AsF_6] with an excess of liquid AsF_5 or with an excess of AsF_5 in HF (see Syntheses of [XeF][MF_6] (M = As, Sb, Bi) and [XeF][M_2F_{11}] (M = Sb, Bi)), and the

stabilities of $As_2F_{11}^-$ salts containing larger, less Lewis acidic counter cations, that is, $(m\text{-}CF_3C_6H_4)(C_6H_5)CF^+$,[35] $(CH_3S)_2CSH^+$,[36] Cl_3PH^+,[37] and Br_3PH^+.[37]

Computational Results. The energy-minimized gas-phase geometries and vibrational frequencies and intensities for the $[XeF][MF_6]$ (M = As, Sb, Bi) ion pairs, were calculated at the PBE1PBE/aug-cc-pVQZ(-PP) and MP2/aug-cc-pVDZ(-PP) levels of theory with all frequencies real (Tables 2 and 4 and Tables S1 and S2 in the Supporting Information). The MP2/aug-cc-pVDZ(-PP) level of theory was chosen because the FIAs had been calculated at this level of theory.[48] Although the analogous krypton salts have been previously calculated,[1] calculations were also carried out in the present study for the krypton analogues at the same levels of theory as their xenon analogues to allow comparisons to be made in the ensuing discussion (Supporting Information, Tables S3−S6). Additional calculations were also performed at different levels of theory for the $[XeF][MF_6]$ ion pairs (Supporting Information, Table S1) to ascertain that the calculated trends were not method dependent. Regardless of the level of theory or the basis set used, the calculated geometrical and frequency trends are similar and consistent. Two starting geometries were used for the $[NgF][MF_6]$ ion pairs, a staggered conformation and an eclipsed conformation. In each case, a staggered energy-minimized geometry was obtained with all vibrational frequencies real (Figure 3 and Figure S2 in the Supporting Information).

(a) Geometries. The calculated $[XeF][MF_6]$ geometries are summarized in Table 2 and in the Supporting Information, Table S1, and those of $[KrF][MF_6]$ are summarized in the Supporting Information, Table S3.

The calculated Ng−F_t bond lengths for the $[NgF][MF_6]$ ion pairs are longer than the experimental values, and both the calculated and the experimental values are not significantly different within their respective series. As expected, the calculated Ng−F_t bond lengths are elongated relative to the calculated bond length of free NgF^+ (Xe, 1.859 (PBE1PBE/Q) and 1.904 (MP2/D) Å; Kr, 1.718 (PBE1PBE/Q) and 1.757 (MP2/D) Å). The calculated Ng---F_b bond lengths are slightly shorter than the experimental bond lengths and are similar in the calculated structures of $[NgF][AsF_6]$ and $[NgF][BiF_6]$, but longer in the calculated structure of $[NgF][SbF_6]$. These trends reflect the more similar FIAs of AsF_5 and BiF_5 and the significantly greater FIA of SbF_5, which are, overall, consistent with the calculated FIA trend $AsF_5 < BiF_5 < SbF_5$.[47,48]

The M−F_2 (M---F_b) bond lengths calculated for $[XeF][MF_6]$ are longer than the average non-bridging M−F bond lengths, and the differences between these bond lengths are slightly greater for $[XeF][MF_6]$ (M = As, Bi) when compared with that of $[XeF][SbF_6]$, in agreement with the observed trends. In all cases, the M−F_3 bond trans to the M−F_2 bond is the shortest, whereas the M−F_4 and M−F_7 bonds that are cis to M−F_2 and closest to the XeF group are the longest. These calculated trends are fully in accord with those observed for $[XeF][AsF_6]$, the only experimental staggered geometry, and for the calculated $[KrF][MF_6]$ ion pairs, which also have staggered conformations (Supporting Information, Table S3).

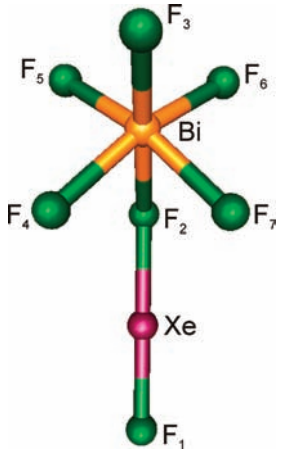

Figure 3. Calculated B3LYP/aug-cc-pVTZ(-PP) gas-phase geometry for $[XeF][BiF_6]$, exemplifying the staggered conformations of the gas-phase $[NgF][MF_6]$ (Ng = Kr, Xe; M = As, Sb, Bi) ion pairs.

In accordance with the experimental[1,2] and calculated structures of the $[KrF][MF_6]$ (M = As, Sb, Bi, Au) analogues, the F_t−Xe---F_b bond angles are also slightly bent in $[XeF][MF_6]$ (M = As, Sb, Bi). Although the many intermolecular Xe···F contacts that occur in the solid state may affect this bond angle, the calculated gas-phase structures of the $[XeF][MF_6]$ (M = As, Sb, Bi) ion pairs also exhibit small distortions from linearity (As, 176.4−177.6°; Sb, 176.1−177.5°; Bi, 176.4−177.9°), suggesting these angles are intrinsic to the ion-pairs.

The calculated Xe---F_b---M bond angles are non-linear for the $[XeF][AsF_6]$ (115.2−122.5°), $[XeF][SbF_6]$ (114.7−122.3°), and $[XeF][BiF_6]$ (114.8−123.0°) ion pairs, showing no dependence on the anion, but are significantly smaller than the experimental values (As, 133.6(2); Sb, 136.9(1); Bi, 156.1(4)°) (see X-ray Crystal Structures). Similar differences have been reported for the crystal structures of $[KrF][MF_6]$ salts,[1] and have been attributed to crystal packing and to long Ng···F contacts that are present in the crystal lattice. The present calculations for the $[KrF][MF_6]$ ion pairs reveal similar differences (Supporting Information, Table S3).

(b) Vibrational Frequencies of $[NgF][MF_6]$ (M = As, Sb, Bi). The vibrational assignments of the $[NgF][MF_6]$ salts are complicated by strong interactions between the anions and the cations, which introduce additional modes associated with the Ng---F_b stretch and the F−Ng---F_b and Ng---F_b---M bends. This interaction also distorts the octahedral geometry of MF_6^-, resulting in an elongated M---F_b bond, which removes the degeneracies of the $\nu_2(E_g)$, $\nu_5(T_{2g})$, $\nu_3(T_{1u})$, $\nu_4(T_{1u})$, and $\nu_6(T_{2u})$ vibrational modes. The anion symmetries of these salts are often assumed to be C_{4v} for the purposes of vibrational assignments; however, the bent Ng---F_b---M bridge bond angles further reduce the symmetries of the ion pairs to C_s (eclipsed and staggered conformations) or C_1 (gauche conformation). The vibrational frequencies and assignments obtained for the $[XeF][MF_6]$ (M = As, Sb, Bi) salts are summarized in Table 4 and in the Supporting Information, Table S2. Only the XeF^+ salts calculated at the PBE1PBE/aug-cc-pVQZ(-PP) level are explicitly discussed because the XeF^+ salts calculated at the MP2 level and the KrF^+ analogues calculated at both levels (in the

Supporting Information, Tables S4−S6) exhibit similar trends.

The Xe−F_t stretching frequencies calculated for the AsF_6^- (600 cm^{-1}), SbF_6^- (609 cm^{-1}), and BiF_6^- (601 cm^{-1}) salts are in very good agreement with the experimental values (As, 607, 611; Sb, 616, 621; Bi, 602, 608 cm^{-1}). The experimental Xe−F_t stretches are very similar, whereas the experimental Xe−F_t bond in [XeF][BiF_6] is significantly longer than the Xe−F_t bonds in [XeF]-[AsF_6] and [XeF][SbF_6], suggesting that there are no clear correlations between the observed Xe−F_t stretching frequencies and Xe−F_t bond lengths. In contrast, the krypton salts reveal an overall correlation of Kr−F_t bond length with Kr−F_t stretching frequency (in the Supporting Information, Tables S4−S6).

The calculations show that the Ng---F_b and M---F_b stretches are coupled in-phase and out-of-phase, with the in-phase mode occurring at lower frequency. This is at variance with the previously published work,[21,22] where the Xe---F_b and M---F_b stretches were described as two uncoupled modes. For [XeF][AsF_6], the two modes occur at 344 and 464 cm^{-1}, respectively, in agreement with the calculated values, 366 and 476 cm^{-1} and for [XeF][SbF_6], these modes occur at 340 and 473/485 cm^{-1}, respectively, in agreement with the calculated values, 353 and 441 cm^{-1}. In the case of [XeF][BiF_6], the in-phase mode is expected to occur at significantly lower frequency (313 cm^{-1}) than those of the [XeF][AsF_6] and [XeF][SbF_6], but was not observed. The out-of-phase mode is observed at 417/439 cm^{-1}, in reasonable agreement with the calculated value, 441 cm^{-1}. Because the Ng---F_b stretches are strongly coupled to the M---F_b stretches, it is not possible to comment on a correlation between Ng---F_b bond lengths and frequencies in the series of NgF^+ salts.

The δ(F_t−Xe---F_b) bending modes occur in the same frequency range, 120 (As), 147 (Sb), and 138 (Bi) cm^{-1}, and are also in agreement with the calculated values (135, 147, and 141 cm^{-1}, respectively). The low vibrational frequencies calculated for the in-plane Xe---F_b---M bending modes (57 (As), 55 (Sb), and 46 (Bi) cm^{-1}) and for the torsional motion of the XeF^+ cation about the F_b---M axis (28 (As), 27 (Sb), and 22 (Bi) cm^{-1}), are consistent with their deformabilities and susceptibilities to crystal packing (see Computational Results; Geometries) as is also the case for the krypton analogues (Supporting Information, Tables S4−S6).

(c) NBO Bond Orders, Valencies, and NPA Charges of [XeF][MF_6]. Further insight into the electronic structures of the [XeF][MF_6] (M = As, Sb, Bi) ion pairs was obtained by the calculation of their NPA (Natural Population Analysis) charges, bond orders, and valencies using the Natural Bond Orbital (NBO) method (Table 5).[49−52] The NBO analyses for the [KrF][MF_6] ion pairs have been calculated at the same level of theory and are reported in the Supporting Information, Table S7.

Table 5. NPA Charges, Valencies, and Bond Orders for [XeF][AsF_6], [XeF][SbF_6], and [XeF][BiF_6] from NBO Analyses

	[XeF][AsF_6]	[XeF][SbF_6]	[XeF][BiF_6]
	NPA Charges and Valencies[a]		
Xe	1.274 [0.564]	1.282 [0.555]	1.271 [0.653]
M	2.670 [3.086]	3.083 [2.319]	2.956 [2.025]
F_1	−0.540 [0.322]	−0.524 [0.329]	−0.533 [0.393]
F_2	−0.589 [0.407]	−0.619 [0.384]	−0.621 [0.403]
$F_{4,7}$	−0.577 [0.475]	−0.659 [0.353]	−0.628 [0.306]
$F_{5,6}$	−0.553 [0.498]	−0.634 [0.365]	−0.601 [0.311]
F_3	−0.555 [0.527]	−0.637 [0.370]	−0.616 [0.316]
	Bond Orders[a]		
Xe−F_1	0.326	0.333	0.386
Xe−F_2	0.217	0.204	0.245
M−F_2	0.243	0.220	0.172
M−$F_{4,7}$	0.552	0.409	0.361
M−$F_{5,6}$	0.574	0.425	0.376
M−F_3	0.590	0.429	0.377
F_1---F_2	−0.003	−0.003	0.007

[a]Bond orders, valencies (in square brackets), and NPA charges were obtained at the PBE1PBE level of theory.

There is little variation among the NPA charges of the atoms that comprise the F_t−Xe---F_b groups of the [XeF][AsF_6] (F_t, −0.540; Xe, 1.274; F_b, −0.589), [XeF]-[SbF_6] (F_t, −0.524; Xe, 1.282; F_b, −0.619), and [XeF]-[BiF_6] (F_t, −0.533; Xe, 1.271; F_b, −0.621) ion pairs as is the case for the krypton analogues: [KrF][AsF_6] (F_t, −0.422; Kr, 1.076; F_b, −0.524), [KrF][SbF_6] (F_t, −0.398; Kr, 1.087; F_b, −0.556), and [KrF][BiF_6] (F_t, −0.410; Kr, 1.075; F_b, −0.554). The charge separations are, however, consistent with Xe−F_t and Xe---F_b bonds that are more ionic than their krypton counterparts. Alternatively, the greater ionic characters of the xenon salts can also be gauged from the sums of the F_t and Xe charges: +0.734 (As), +0.758 (Sb), and +0.738 (Bi) which are closer to the +1 charge expected for a free NgF^+ cation than those found for the [KrF][MF_6] ion pairs where the corresponding sums are +0.654 (As), +0.689 (Sb), and +0.665 (Bi). The greater cation−anion charge separations in the XeF^+ salts (where F_bMF_5 group charge sums are equal, but opposite in sign, to those of NgF_t) indicate that the [XeF]-[MF_6] ion pairs are more ionic than the [KrF][MF_6] ion pairs, and are consistent with the shorter M---F_b distances calculated for the XeF^+ salts (Table 2 and in the Supporting Information, Table S1). These findings are corroborated by the X-ray crystal structures and calculated geometries of [$BrOF_2$][AsF_6]·2NgF_2.[26,53] The contact distances between bromine and XeF_2 are shorter when compared with those of the KrF_2 analogue, which is consistent with the greater ionic character of the Xe−F bonds in XeF_2. The observation is also supported by the experimental and calculated vibrational frequencies, by NBO and ELF analyses, and by the calculated fluoride ion donor strengths for KrF_2 and XeF_2 in the aforementioned work. The fluoride ion donor strengths have been recalculated in the present work at the PBE1PBE/aug-cc-pVQZ(-PP) and MP2/aug-cc-pVDZ(-PP) levels of

(49) Reed, A. E.; Weinstock, R. B.; Weinhold, F. *J. Chem. Phys.* **1985**, *83*, 735–746.
(50) Reed, A. E.; Curtiss, L. A.; Weinhold, F. *Chem. Rev.* **1998**, *88*, 899–926.
(51) Glendening, E. D.; Reed, A. E.; Carpenter, J. E.; Weinhold, F. *NBO*, Version 3.1; Gaussian Inc.: Pittsburgh, PA, 1990.
(52) Glendening, E. D.; Badenhoop, J. K.; Reed, A. E.; Carpenter, J. E.; Bohmann, C. M.; Morales, C. M.; Weinhold, F. *NBO*, Version 5.0; Theoretical Chemistry Institute, University of Wisconsin: Madison, WI, 2001.
(53) Brock, D. S.; Casalis de Pury, J. J.; Mercier, H. P. A.; Schrobilgen, G. J.; Silvi, B. *J. Am. Chem. Soc.* **2010**, *132*, 3533–3542.

theory for $NgF_{2(g)} \rightarrow NgF^{+}_{(g)} + F^{-}_{(g)}$, giving 937.9, 903.2 kJ mol^{-1}, respectively, for XeF_2 and 963.9, 944.4 kJ mol^{-1}, respectively, for KrF_2.

The greater ionic characters of the xenon(II) salts have negligible effects on the pnictogen charges of the anions (As, 2.670; Sb, 3.083; Bi, 2.956), with very similar values for the $[KrF][MF_6]$ salts (As, 2.661; Sb, 3.075; Bi, 2.949). In both series, the pnictogen charge trend parallels the FIA trend for the parent pentafluoride. Consistent with a more ionic $[XeF][MF_6]$ series, the average fluorine ligand charges of the MF_6^- anions are somewhat more negative in the XeF^+ salts (As, −0.567; Sb, −0.640; Bi, −0.616) than in the KrF^+ salts (As, −0.552.; Sb, −0.628; Bi, −0.602).

The $Xe-F_t$ and $Xe\text{---}F_b$ bond orders do not vary significantly from one salt to another. The $Xe-F_t$ bond orders (As, 0.326; Sb, 0.333; Bi, 0.386) are about 1.6 times greater than the $Xe\text{---}F_b$ bond orders (As, 0.217; Sb, 0.204; Bi, 0.245), which is consistent with the shorter $Xe-F_t$ bond lengths. The Xe−F bond orders are comparable to the $Kr-F_t$ (As, 0.344; Sb, 0.356; Bi, 0.335) and $Kr\text{---}F_b$ (As, 0.210; Sb, 0.201; Bi, 0.212) bond orders calculated for the $[KrF][MF_6]$ salts in the present work (in the Supporting Information, Table S7).

With the exception of $[XeF][BiF_6]$, the xenon valencies exhibit little variation among the $[XeF][MF_6]$ salts (As, 0.564; Sb, 0.555; Bi, 0.653) and are comparable to those calculated for the krypton in the $[KrF][MF_6]$ ion pairs (As, 0.572; Sb, 0.582; Bi, 0.554). The pnictogen valencies of the xenon salts (As, 3.086; Sb, 2.319; Bi, 2.025) are nearly identical to those of the krypton analogues (As, 3.080; Sb, 2.316; Bi, 2.017).

Thermochemistry of Noble-Gas Fluorocation Salts. It is important that this section of the paper be read in conjunction with the section entitled "Thermochemical Study of Noble-Gas Fluorocation Salts" in the Supporting Information. Experimental determination of thermochemical data such as the standard enthalpy of formation, $\Delta_f H^o$, standard free energy of formation, $\Delta_f G^o$, and standard entropy, S^o, has not featured prominently in the development of noble-gas chemistry because the compounds are highly reactive oxidizers and highly air sensitive. The resulting shortfall of information may be addressed by employing VBT, which had its origins in the work of Mallouk and Bartlett[16] and was developed, over a decade later, in a series of papers by Jenkins and co-workers[17−20] to estimate missing thermodynamic data for the solid state. This is the theme of the thermochemistry section of this paper. Details, together with 13 clarifying examples, of the use of VBT are to be found in the Supporting Information.

In the VBT approach, the relationships between lattice energy, U_{POT} (eq 3), and standard entropy, S^o_{298} (eq 4), of a solid material and the corresponding molecular (formula unit) volume, V_m, are invoked

$$U_{POT} \approx 2I[\alpha(V_m)^{-1/3} + \beta] \quad (3)$$

where I is the ionic strength[54] of the lattice, $I = \frac{1}{2}\sum n_i z_i^2$, where n_i is the number of ions having the charge z_i (the summation extending over the formula unit), α and β are the stoichiometrically dependent coefficients[55] given in Table 1 of ref 17.

$$S^o_{298} = kV_m + c \quad (4)$$

where k and c are constants.[56]

In conjunction with gas-phase ion formation data, Born−Fajans−Haber cycles are constructed to estimate $\Delta_f H^o$ for the salts in question and hence the standard free energy of formation, $\Delta_f G^o$ can then be estimated. All lattice energies, enthalpies, and Gibbs free energies are in units of kJ mol^{-1} and entropies are in J K^{-1} mol^{-1} and V_m, determined from the crystallographic unit cell, is in nm^3 in the ensuing discussion.

(a) Volume, V_m, Estimation for Salts. Table 6 gives the results generated from VBT which, when used in conjunction with available experimentally determined, as well as calculated, thermodynamic data for the associated gaseous ions, leads to the estimated standard thermodynamic data shown in columns 10−14 for the compounds listed. Column 3 of Table 6 lists details of the unit cell volumes, V_{cell}, and Z-values from various crystal structure determinations. Values are further presented for hypothetical ArF^+ salts using an estimate for $V_+(ArF^+)$ derived from thermochemical arguments given in the Supporting Information.

All the salts containing the $Kr_2F_3^+$ cation that have been studied crystallographically contain adducted KrF_2 or $[KrF][AsF_6]$ and do not permit direct determination of $V_+(Kr_2F_3^+)$. However, using the known volumes of KrF_2 (0.0567 nm^3) and SbF_6^- (0.121(12) nm^3), $V_+(Kr_2F_3^+)$ is estimated to be 0.083 nm^3 based on the structures of $[Kr_2F_3][SbF_6]$ and $[Kr_2F_3]_2[SbF_6]_2 \cdot KrF_2$. Using this volume for $Kr_2F_3^+$, the formula unit volumes of $[Kr_2F_3][SbF_6]$ and $[Kr_2F_3][AsF_6]$

(54) Glasser, L. *Inorg. Chem.* **1995**, *34*, 4935–4938.
(55) For a MX (1:1) salt, like the majority considered in this paper, the parameters α and β in eq 3 are 117.3 kJ mol^{-1} nm and 51.9 kJ mol^{-1}, respectively, and the ionic strength $I = 1$.
(56) In eq 4, k = 1360 J K^{-1} mol^{-1} nm^{-3} and c = 15 J K^{-1} mol^{-1}.

(57) Sladky, F. O.; Bulliner, P. A.; Bartlett, N.; DeBoer, B. G.; Zalkin, A. *Chem. Commun.* **1968**, 1048–1049.
(58) McKee, D.; Adams, C. J.; Bartlett, N. *Inorg. Chem.* **1973**, *12*, 1722–1725.
(59) Boldrini, P.; Gillespie, R. J.; Ireland, P. R.; Schrobilgen, G. J. *Inorg. Chem.* **1974**, *13*, 1690–1694.
(60) Gillespie, R. J.; Martin, D.; Schrobilgen, G. J.; Slim., D. R. *J. Chem. Soc., Dalton Trans.* **1977**, 2234–2237.
(61) McKee, D. E.; Adams, C. J.; Zalkin, A.; Bartlett, N. *J. Chem. Soc., Chem. Comm.* **1973**, 26–28.
(62) Mercier, H. P. A.; Sanders, J. C. P.; Schrobilgen, G. J.; Tsai, S. *Inorg. Chem.* **1993**, *32*, 145–151.
(63) Bartlett, N.; Wechsberg, M. *Z. Allg. Anorg. Chem.* **1971**, *385*, 5–17.
(64) Leary, K.; Templeton, D. H.; Zalkin, A.; Bartlett, N. *Inorg. Chem.* **1973**, *12*, 1726–1730.
(65) Drews, T.; Seppelt, K. *Angew. Chem., Int. Ed. Engl.* **1997**, *36*, 273–274.
(66) Fir, B. A.; Gerken, M.; Pointner, B. E.; Mercier, H. P. A.; Dixon, D. A.; Schrobilgen, G. J. *J. Fluorine Chem.* **2000**, *105*, 159–167.
(67) Leary, K.; Zalkin, A.; Bartlett, N. *J. Chem. Soc., Chem. Comm.* **1973**, 131–132.
(68) Benkic, P.; Golic, L.; Koller, J.; Žemva, B. *Acta. Chim. Slov.* **1999**, *46*, 239–252.
(69) Jesih, A.; Luter, K.; Leban, I.; Žemva, B. *Inorg. Chem.* **1989**, *28*, 2911–2914.
(70) Gillespie, R. J.; Martin, D.; Schrobilgen, G. J.; Slim., D. R. *J. Chem. Soc., Dalton Trans.* **1977**, 1003–1006.
(71) Faggiani, R.; Kennepohl, D. K.; Lock, C. J. L.; Schrobilgen, G. J. *Inorg. Chem.* **1986**, *25*, 563–571.
(72) Fir, B. A.; Mercier, H. P. A.; Sanders, J. C. P.; Dixon, D. A.; Schrobilgen, G. J. *J. Fluorine Chem.* **2001**, *110*, 89–107.
(73) Hellwege, K.-H., Hellwege, A. M., Eds.; *Crystal Structure data for Inorganic Compounds*; Landolt-Bornstein series; Springer-Verlag: Berlin, 1993.
(74) Latimer, W. M. *Oxidation Potentials*, 2nd ed.; Prentice Hall: Englewood Cliffs, NJ, 1961; Appendix III, p 359.
(75) Latimer, W. M. *J. Am. Chem. Soc.* **1921**, *43*, 818–826.
(76) Jenkins, H. D. B.; Glasser, L. *Inorg. Chem.* **2003**, *42*, 8702–8708.

Table 6. Crystal Structure Data, Ion Volumes, V_+, V_-, VBT Lattice Energies, U_{POT}, Enthalpies of Formation, $\Delta_f H^o$, VBT Standard Entropies, S^o_{298}, Standard Entropies of Formation, $\Delta_f S^o$ and Gibbs Energies of Formation, $\Delta_f G^o$ for XeF^+,[a] XeF_3^+,[b] $XeOF_3^+$,[c] XeF_5^+,[d] Xe_2^+,[e] $Xe_2F_3^+$,[f] $Xe_2F_{11}^+$,[g] FXeOS(F)OXeF$^+$,[h] $XeN(SO_2F_2)_2^+$,[i] $XeOSeF_5^+$,[j] $XeOTeF_5^+$,[j] $XeCl^+$ [k] Salts; KrF^+ [l] and $Kr_2F_3^+$ [m] Salts (and in Addition for KrF_2 [m]) and for Hypothetical ArF^+ Salts as Listed

salt	ref	V_{cell} nm^3	Z	V_m nm^3	V_- nm^3	V_+ nm^3	I	U_{POT} kJ mol^{-1}	$\Delta_f H^o$ kJ mol^{-1}	S^o_{298}, J K^{-1} mol^{-1} L[n]	S^o_{298}, J K^{-1} mol^{-1} JG[o]	$\Delta_f S^o$ J K^{-1} mol^{-1}	$\Delta_f G^o$ [p] kJ mol^{-1}
XeF_2									−133.9[q]				−62.8[q]
$[XeF][BF_4]$[r]				0.112[r]			1	590	−1246		167	−516	−1092(15)[s]
$[XeF][PF_6]$	57	0.5668	4	0.1417	0.109(8)	0.033	1	544	−1718(2)	213	208	−712	−1506(2)
$[XeF][AsF_6]$	this work	0.59582	4	0.1490	0.110(7)	0.039	1	546	−1409(22)	222	218	−696	−1202(22)
$[XeF][AsF_6]$	8	0.6247	4	0.1562	0.110(7)	0.046	1	558	−1421	222	227	−688	−1215(15)[s]
$[XeF][SbF_6]$	this work	0.63620	4	0.1591	0.121(12)	0.038	1	537	−1568(52)	229	231	−694	−1361(52)
$[XeF][SbF_6]$		0.6396	4	0.1599	0.121(12)	0.035	1	536	−1567	229	232	−693	−1360[s]
$[XeF][BiF_6]$	this work	0.64201	4	0.1605	0.124	0.037	1	536		239	233	−703	
$[XeF][RuF_6]$	7	0.6422	4	0.1606	0.116	0.045	1	535		226	233	−675	
$[XeF][As_2F_{11}]$[r]				0.242[r]			1	480(4)	−2670		344	−1110	−2339(15)[s]
$[XeF][Sb_2F_{11}]$	this work	0.52437	2	0.2622	0.227(20)	0.035	1	470	−2945(63)	418	372	−1101	−2618(63)
$[XeF][Sb_2F_{11}]$	10	0.5435	2	0.2718	0.227(20)	0.045	1	466	−2942	418	385	−1093	
$[XeF][Bi_2F_{11}]$	this work	1.04482	4	0.2612	0.222[b]	0.039	1	471		438	370	−1130	
$[XeF_3][BF_4]$[r]				0.129[r]			1	568	−1329		190	−526	−1172(13)
$[XeF_3]PF_6]$[r]				0.165[r]			1	532	−1812		239	−884	
$[XeF_3][AsF_6]$[r]				0.166[r]			1	531	−1500(26)		241	−876	−1239(26)
$[XeF_3][SbF_6]$	58	0.7433	4	0.1858	0.121(12)	0.065	1	515	−1652(54)	262	259	−869	−1393(54)
$[XeF_3][SbF_6]$	59	0.71785	4	0.1795	0.121(12)	0.058	1	520	−1657(54)	262	259	−869	−1398(54)
$[XeF_3][BiF_6]$	60	0.3637	2	0.1819	0.124	0.058	1	518		273	311	−828	
$[XeF_3][As_2F_{11}]$[r]				0.261[r]		0.056(15)	1	471(5)	−2767		370	−1289	−2383(15)[s]
$[XeF_3][Sb_2F_{11}]$	45, 61	0.5148	2	0.2574	0.227(20)	0.030	1	472	−3054	460	365	−1316	−2661(15)[s]
$[XeF_3][Sb_2F_{11}]$	this work	0.5439	2	0.2675	0.227(20)	0.041	1	468	−3050	460	369	−1312	−2659(15)[s]
$[XeOF_3][SbF_6]$	62	0.7634	4	0.1909	0.121(12)	0.070	1	511		275	275	−956	
$[XeF_5][BF_4]$				0.150[r]			1	545	−1492		219	−869	−1233(46)
$[XeF_5][PF_6]$[r]				0.186[r]			1	515	−1981		268	−1058	−1666(46)
$[XeF_5][AsF_6]$	63	0.7844	4	0.1961	0.110(7)	0.086	1	508	−1663(51)	288	282	−1038	−1354(51)
$[XeF_5][SbF_6]$[r]				0.198[r]			1	506	−1829		284	−1047	
$[XeF_5][RuF_6]$	7	0.77303	4	0.1933	0.116	0.077	1	510		293	278	−1036	
$[XeF_5]_2[PdF_6]$	64	1.1229	4	0.2807	0.143	0.069	3	1336		425	397	−1602	
$[XeF_5][Sb_2F_{11}]$[r]				0.304[r]			1	453	−3221		428	−1455	−2787(78)
$[XeF_5][Bi_2F_{11}]$[r]				0.299[r]			1	455			422	−1127	
$[Xe_2][Sb_4F_{21}]$	65	0.9736	2	0.4868	0.409	0.078	1	402		774	677	−1975	
$[Xe_2F_3][AsF_6]$	63	0.69815	3	0.2327	0.110(7)	0.123	1	485		312	331	−956	
$[Xe_2F_3][AsF_6]$	57	2.7993	1	0.2333	0.110(7)	0.123	1	486		312	332	−955	
$[Xe_2F_3][AsF_6]$	66	2.7169[e]	1	0.2264	0.110(7)	0.116	1	489		312	323	−964	
$[Xe_2F_3][AsF_6]$	66	0.6834[f]	3	0.2278	0.110(7)	0.118	1	488		312	325	−962	
$[Xe_2F_3][SbF_6]$	66	0.8998	3	0.2250	0.121(12)	0.104	1	490		319	321	−978	
$[Xe_2F_{11}][AuF_6]$	67	1.224	4	0.3060	0.105	0.191	1	452		462	431	−1680	
$[Xe_2F_{11}][VF_6]$	68	1.1925	4	0.2981	0.112	0.186	1	455		440	420	−1672	
$[Xe_2F_{11}]_2[NiF_6]$	69	1.9542	4	0.4886	0.126	0.181	3	1080		823	679	−2869	
[FXeOS(F)OXeF] $[AsF_6]$[n]	70	1.132	4	0.2830	0.110	0.173	1	461		373	400		
$[XeN(SO_2F_2)_2]$ $[Sb_3F_{16}]$	71	1.8872	4	0.4718	0.317	0.155	1	405		682	657		
$[XeOSeF_5][AsF_6]$	72	0.4880	2	0.2440	0.110(7)	0.134	1	479		350	347	−1118	
$[XeOTeF_5][AsF_6]$	72	0.5204	2	0.2602	0.110(7)	0.150	1	471		357	369	−1242	
$[XeCl][Sb_2F_{11}]$	46	2.2639	8	0.2829	0.227	0.056	1	461		439	390	−1271	
α-KrF_2	73	0.11332	2	0.0567						97	92	−275	
$[KrF][BF_4]$[r]				0.103[r]			1	604	−1026		155	−522	
$[KrF][PF_6]$[r]				0.139[r]			1	557	−1498		204	−711	−1286(15)[s]
β-$[KrF][AsF_6]$	1	0.55602	4	0.1390	0.110(7)	0.029	1	556	−1186	216	204	−704	−976(15)[s]
$[KrF][SbF_6]$	1	0.59473	4	0.1487	0.121(12)	0.028	1	546	−1342	223	217	−699	−1134(15)[s]
$[KrF][BiF_6]$	1	0.6176	4	0.1544	0.124	0.030	1	541		233	225	−705	
$[KrF][AuF_6]$	2	0.5848	4	0.1462	0.115	0.031	1	549		232	214	−707	
$[KrF][Sb_2F_{11}]$	1			0.257[r]			1	473	−2716		365	−1107	−2386(15)[s]
$[Kr_2F_3][SbF_6]\cdot KrF_2$	1	0.5171	2	0.2586	0.121(12)	0.081					366	−1287	
$[Kr_2F_3]_2[SbF_6]_2\cdot KrF_2$	1	1.8701	4	0.4675	0.121(12)	0.084					651	−2289	
$[Kr_2F_3][AsF_6]\cdot$[KrF] $[AsF_6]$	1	1.3676	4	0.3419	0.110(7)	0.092					480	−1705	
$[Kr_2F_3][PF_6]$[r]				0.192[r]			1	510			276	−1006	
$[Kr_2F_3][AsF_6]$[r]				0.193[r]			1	510			277	−999	
$[Kr_2F_3][SbF_6]$[r]				0.204[r]			1	502			292	−995	
$[Kr_2F_3][BiF_6]$[r]				0.207[r]			1	500			297	−1001	
$[ArF][BF_4]$				0.096[r]	0.073	0.023	1	616	−921		145	−523	−765(15)[s]

Table 6. Continued

salt	ref	V_{cell} nm^3	Z	V_m nm^3	V_- nm^3	V_+ nm^3	I	U_{POT} kJ mol^{-1}	$\Delta_f H^o$ kJ mol^{-1}	S^o_{298}, J K^{-1} mol^{-1} L^n	S^o_{298}, J K^{-1} mol^{-1} JG^o	$\Delta_f S^o$ J K^{-1} mol^{-1}	$\Delta_f G^{o\,p}$ kJ mol^{-1}
$[ArF][PF_6]^r$				0.132(8)^v	0.109(8)	0.023	1	564(8)	−1387		195	−711	−1175(15)^s
$[ArF][AsF_6]^r$				0.133(7)^r	0.110(7)	0.023	1	563(7)	−1075		195	−705	−865(15)^s
$[ArF][SbF_6]^r$				0.144(12)^r	0.121(12)	0.023	1	551(11)	−1232(53)		211	−699	−1024(15)^s
$[ArF][AuF_6]^r$				0.138(14)^r	0.115(14)	0.023	1	558(15)			203	−709	
$[ArF][Sb_2F_{11}]^r$				0.250(9)^r	0.227(20)	0.023	1	476(9)	−2602		355	−1108	−2272(15)^s
$[ArF][Sb_3F_{16}]^r$				0.340(21)^r	0.317(21)	0.023	1	440(7)			477		

[a] From refs 7, 8, 10, 57. [b] From refs 45, 58−61. [c] From ref 62. [d] From refs 7, 63, 64. [e] From ref 65. [f] From refs 63−66. [g] From refs 67−69. [h] From ref 70. [i] From ref 71. [j] From ref 72. [k] From ref 46. [l] From refs 1, 73. [m] From ref 73. [n] Standard entropy, S^o_{298}, calculated using Latimer's Rules (from refs 74, 75) (see Supporting Information for details and examples). [o] Standard entropy, S^o_{298} calculated using Jenkins and Glasser's equation (from refs 17, 19, 76): $S^o_{298} = 1360V_m + 15$. (See Supporting Information for details and examples). [p] $\Delta_f G^o = \Delta_f H^o - T\Delta_f S^o$. [q] Taken from Ellis, H.; Ed. Revised Nuffield Advance Science Book of Data, Nuffield-Chelsea Curriculum Trust, Longman Group Ltd., 3rd Impression, 1985. [r] Salts which are currently unknown, hypothetical or known salts for which volume V_m or density ρ are unknown. Thermochemical values (columns 9−14) are estimated on the basis of V_m predicted from ion volumes using anion data, V_- (from ref 17) and average cation volumes, V_+, established by averaging data in this table to be: $V_+(XeF^+)$ = 0.039(8); $V_+(XeF_3^+)$ = 0.056(15); $V_+(XeF_5^+)$ = 0.077(9); $V_+(Xe_2F_3^+)$ = 0.117(6); $V_+(Xe_2F_{11}^+)$ = 0.186(5); $V_+(XeOF_3^+)$ = 0.070; $V_+(Xe_2^+)$ = 0.078; $V_+(FXeOS(F)OXeF^+)$ = 0.173; $V_+(XeN(SO_2F_2)_2^+)$ = 0.155; $V_+(XeOSeF_5^+)$ = 0.134; $V_+(XeOTeF_5^+)$ = 0.150; $V_+(XeCl^+)$ = 0.056; $V_+(KrF^+)$ = 0.030(2); $V_+(Kr_2F_3^+)$ = 0.083(2) nm^3. In the case of argon compounds, as explained in the text, $V_+(ArF^+)$ is taken to be approximately that of the ion KF^+ and equal to 0.023 nm^3. [s] Where specific errors have not been estimated, a global error of ±15 kJ mol^{-1} is assumed for VBT calculations.

can be further estimated and used to calculate the lattice energies of these and other simple salts. Examples of volume calculation and estimation are given in the Supporting Information (Examples 1−5).

(b) Lattice Energies, U_{POT}, for Noble-Gas Cation Salts Estimated from Volume Data. The lattice energies calculated from the VBT approach are summarized in Table 6 and decrease as V_m increases, as expected based on the inverse cube root dependence of the volume shown in eq 3. Larger lattice energies (kJ mol^{-1}) are noted for the BF_4^- salts (ArF^+, 616; KrF^+, 604; XeF^+, 590), while salts containing particularly large cations ($[Xe_2F_{11}][AuF_6]$, 462) or anions ($[XeN(SO_2F_2)_2][Sb_3F_{16}]$, 405) have notably lower lattice energies. The exceptions to this trend are clearly $[XeF_5]_2[PdF_6]$ (1336 kJ mol^{-1}) and $[Xe_2F_{11}]_2[NiF_6]$ (1080 kJ mol^{-1}) where the higher ionic strengths of these salts (I = 3) have a greater influence on the lattice energy than V_m does. It is noteworthy that for a given anion (i.e., SbF_6^-), the lattice energy (Table 6) generally does not change appreciably when the cation is mononuclear with respect to the noble gas and is varied (i.e., XeF^+, 536; XeF_3^+, 515; XeF_5^+, 506; $XeOF_3^+$, 511; KrF^+, 546; ArF^+, 551). This reflects the general observation that these cation volumes are usually small, and that the volume of the anion dominates crystal packing and V_m. Examples of lattice energy estimations are provided in the Supporting Information (Examples 6 and 7).

(c) Standard Enthalpy of Formation, $\Delta_f H^o$, Estimation for Noble-Gas Cation Salts. The enthalpy of formation for the salt can be estimated if the $\Delta_f H^o$ values of the constituent gaseous ions are established. Standard enthalpies of formation for the noble-gas cations have estimated values, as follows: ArF^+ = 1398 kJ mol^{-1} (taken from the estimate for the dissociation energy of $ArF^+(g)$ into $Ar^+(g)$ and $F_2(g)$ of 205(13) kJ mol^{-1} [77] and using $\Delta_f H^o(F,g)$ = 78.9 kJ mol^{-1} [78]); KrF^+ = 1281 (calculated from the F^+ detachment energy[77]); XeF^+ = 1048 (calculated from the fluoride ion donation energy[79]); XeF^+ = 1076(2) (calculated from the F^+ detachment energy[77]); XeF_3^+ = 943 (calculated from the fluoride ion donation energy;[79] XeF_3^+ = 1021 (calculated from the F^+ detachment energy[77]); XeF_5^+ = 757 (calculated from the fluoride ion donation energy;[79] and XeF_5^+ = 879 (calculated from the F^+ detachment energy[77]). The standard enthalpies of formation determined for several known and unknown noble-gas containing salts using the fluoride ion donation energy[79] found in Table 6, column 10. These values were used because it was felt that they have a firmer experimental basis than the detachment values.

Although experimental results are scarce for the noble-gas containing salts, experimental enthalpies of reaction have been measured for the reactions of XeF_2 with SbF_5, yielding $[XeF][SbF_6]$ (ΔH^o_{react}, −32 kJ mol^{-1})[80] and $[XeF][Sb_2F_{11}]$ (ΔH^o_{react}, −58(21),[10] −99[80] kJ mol^{-1}). Combining these enthalpies of reaction with the standard enthalpies of formation known for XeF_2 (−162.76(88) kJ mol^{-1})[6] and SbF_5 (l) (−1328(12) kJ mol^{-1}),[80] the standard enthalpies of formation of $[XeF][SbF_6]$ and $[XeF][Sb_2F_{11}]$ are estimated to be −1523(12) and −2949(21) kJ mol^{-1}, respectively. These values are very similar to those (independently) determined for $[XeF][SbF_6]$ (−1568(52) kJ mol^{-1}) and $[XeF][Sb_2F_{11}]$ (−2945(63) kJ mol^{-1}) using a VBT calculation for U_{POT} (Table 6) coupled with the known enthalpies of formation for XeF^+,[77,79] SbF_6^-,[81,82] and $Sb_2F_{11}^-$.[81,82] The excellent agreement between these two methods of determining $\Delta_f H^o$ for $[XeF][SbF_6]$ and $[XeF][Sb_2F_{11}]$ suggests that the VBT approach can be applied with reasonable confidence to the noble-gas salts in cases where more traditional calorimetric results are either not available or experimentally impractical.

(77) Frenking, G.; Koch, W.; Deakyne, C. A.; Liebman, J. F.; Bartlett, N. *J. Am. Chem. Soc.* **1989**, *111*, 31–33.
(78) Wagman, D. D.; Evans, W. H.; Parker, V. B.; Schumm, R. H.; Halow, I.; Bailey, S, M.; Churney, K. L.; Nuttall, R. L. *N.B.S. Tables of Chemical Thermodynamic Properties*; Selected Values for Inorganic, C1, and C2 Organic Substances in SI units. *J. Phys. Chem. Ref. Data*, *11*, Supplement No. 2, **1982**, 1−392.
(79) Berkowitz, J.; Chupka, W. A.; Guyin, P. M.; Holloway, J. H.; Spohr, R. *J. Phys. Chem.* **1971**, *75*, 1461–1465.
(80) Burgess, J.; Peacock, R. D.; Sherry, R. J. *J. Fluorine Chem.* **1982**, *20*, 541–554.
(81) Jenkins, H. D. B.; Roobottom, H. K.; Passmore, J. *Inorg. Chem.* **2003**, *42*, 2886–2893.
(82) Jenkins, H. D. B.; Krossing, I.; Passmore, J.; Raabe, I. *J. Fluorine Chem.* **2004**, *125*, 1585–1592.

The trends observed in the predicted $\Delta_f H^o$ values are such that for XeF_n^+ salts they fall in the orders:

$$(n = 1)\ [XeF][BF_4] > [XeF][AsF_6] > [XeF][SbF_6] > [XeF][PF_6] \gg [XeF][As_2F_{11}] > [XeF][Sb_2F_{11}]$$

$$(n = 3)\ [XeF_3][AsF_6] > [XeF_3][SbF_6] \gg [XeF_3][As_2F_{11}] > [XeF_3][Sb_2F_{11}]$$

$$(n = 5)\ [XeF_5][BF_4] > [XeF_5][As\ F_6] > [XeF_5][PF_6] \gg [XeF_5][Sb_2F_{11}]$$

with a similar order observed for the KrF^+ salts:

$$[KrF][AsF_6] > [KrF][SbF_6] > [KrF][PF_6] \gg [KrF][Sb_2F_{11}]$$

Salts having the same anion have broadly similar values for $\Delta_f H^o$, to within 100−200 kJ mol^{-1}. Example 8 in the Supporting Information further illustrates the calculation.

(d) Standard Entropy, S^o_{298}, Estimation and Standard Entropy of Formation, $\Delta_f S^o$. There are two simple approaches to estimating S^o_{298} for a salt (columns 11 and 12 labeled *n* and *o* in Table 6) which give similar values. The Latimer approach[74,75] combines elemental entropy values for the compound additively, whereas the Jenkins and Glasser[76] approach uses V_m values taken directly from crystal structure determinations. For a given cation, as the anion size increases, the value of S^o_{298} also increases. The standard entropy of formation of the salt from its elements in their standard states, $\Delta_f S^o$, is calculated directly from S^o_{298} for the salt, after combination with standard thermochemical values[78] for S^o_{298}(Ng, g), S^o_{298}(M, s), and $S^o_{298}(F_2, g)$ where M = B, P, As, Sb, and so forth. The results for $\Delta_f S^o$ are listed in column 13, Table 6. Examples 9−11 and Example 12, in the Supporting Information, further illustrate the calculation of S^o_{298} and $\Delta_f S^o$, respectively.

(e) Standard Free Energy of Formation, $\Delta_f G^o$. The value for $\Delta_f G^o$ may be calculated once $\Delta_f S^o$ and $\Delta_f H^o$ have been estimated using the standard relationship. Trends found for $\Delta_f G^o$ are broadly similar to those indicated above for $\Delta_f H^o$, with magnitudes increased (so becoming less negative) by about 200 kJ mol^{-1} in most cases (see column 14, Table 6). Example 13 in the Supporting Information further illustrates the calculation.

(f) Application of VBT to Establish the Thermochemistries of Noble-Gas Salts. A series of predictions and validations follow for noble-gas compounds using VBT which illustrate the usefulness of this approach in cases where traditional thermochemistry is unavailable.

(i) VBT Used to Examine the Syntheses of $[XeF][MF_6]$, $[XeF][M_2F_{11}]$, $[XeF_3][MF_6]$, and $[XeF_3][M_2F_{11}]$ from XeF_2, XeF_4, and MF_5 (M = As, Sb). The salts, $[XeF][SbF_6]$, $[XeF][Sb_2F_{11}]$, $[XeF_3][SbF_6]$ and $[XeF_3][Sb_2F_{11}]$ are known to be stable and are predicted to be so using VBT. Their preparative reactions, 5−8, follow:

$$XeF_2(s) + SbF_5(l) \rightarrow [XeF][SbF_6](s) \quad (5)$$

$$XeF_4(s) + SbF_5(l) \rightarrow [XeF_3][SbF_6](s) \quad (6)$$

$$XeF_2(s) + 2SbF_5(l) \rightarrow [XeF][Sb_2F_{11}](s) \quad (7)$$

$$XeF_4(s) + 2SbF_5(l) \rightarrow [XeF_3][Sb_2F_{11}](s) \quad (8)$$

Although a value for $\Delta_f H^o(SbF_5, g) = -1301$ kJ mol^{-1} has been established,[80] there is no value in the literature for $\Delta_f G^o(SbF_5, g)$. However, $\Delta_f G^o(SbF_5, l) = -1242$ kJ mol^{-1} has been reported.[83] Using the data calculated from VBT given in Table 6:

$$\Delta G(5) = \Delta_f G^o([XeF][SbF_6], s) - \Delta_f G^o(XeF_2, s) - \Delta_f G^o(SbF_5, l) \approx -1361(52) - (-63) - (-1242) = -56(52)\ \text{kJ mol}^{-1} \quad (9)$$

taking $\Delta_f G^o(XeF_2, s) = -62.8$ kJ mol^{-1};[84]

$$\Delta G(6) = \Delta_f G^o([XeF_3][SbF_6], s) - \Delta_f G^o(XeF_4, s) - \Delta_f G^o(SbF_5, l) \approx -1393(54) - (-121) - (-1242) = -30(54)\ \text{kJ mol}^{-1} \quad (10)$$

taking $\Delta_f G^o(XeF_4, s) = -121.3$ kJ mol^{-1};[84]

$$\Delta G(7) = \Delta_f G^o([XeF][Sb_2F_{11}], s) - \Delta_f G^o(XeF_2, s) - 2\Delta_f G^o(SbF_5, l) \approx -2618(63) - (-63) - 2(-1242) = -71(63)\ \text{kJ mol}^{-1} \quad (11)$$

$$\Delta G(8) = \Delta_f G^o([XeF_3][Sb_2F_{11}], s) - \Delta_f G^o(XeF_4, s) - 2\Delta_f G^o(SbF_5, l) \approx -2660(15) - (-121) - 2(-1242) = -55(15)\ \text{kJ mol}^{-1} \quad (12)$$

the gross thermodynamic stabilities of the four salts above are therefore correctly predicted by VBT.

In the case of As analogues of the above salts, the thermodynamics turn out to be much harder to quantify by VBT since key thermodynamic data (i.e., $\Delta_f G^o(AsF_5, l)$) are unavailable experimentally. While this frustrates the use of VBT in the absence of so much experimental data, the present VBT calculations have shown that adoption of a value $\Delta_f G^o(AsF_5, l) \approx -1138$ kJ mol^{-1} appears to be consistent with much of the observed thermochemistry and stabilities, although it predicts highly borderline thermodynamics in most cases. The large errors found in the calculated ΔG values confirm that improved experimental thermodynamics is really the only answer here. Thus, $[XeF][AsF_6]$ is an established stable salt synthesized by

(83) Taking the value for $\Delta_f H^o(SbF_5, l) = -1328$ kJ mol^{-1} (ref 80) and the standard entropy, $S^o_{298}(SbF_5, l) = 265$ J K^{-1} mol^{-1} (Nagarajan, G. *Bull. Soc. Chim. Belg.* **1962**, *71*, 324–328) one can establish the standard entropy of formation: $\Delta_f S^o(SbF_5, l) = -288$ J K^{-1} mol^{-1} and thus; $\Delta_f G^o(SbF_5, l) = -1242$ kJ mol^{-1}.

(84) Ellis, H., Ed.; *Revised Nuffield Advanced Science Book of Data*; Nuffield-Chelsea Curriculum Trust, Longman Group Ltd., 3rd Impression, 1985.

reaction 13

$$XeF_2(s) + AsF_5(l) \rightarrow [XeF][AsF_6](s) \quad (13)$$

for which (assuming the value of $\Delta_f G^o(AsF_5, l)$ above)

$$\Delta G(13) = \Delta_f G^o([XeF][AsF_6], s) - \Delta_f G^o(XeF_2, s) - \Delta_f G^o(AsF_5, l) \approx -1202(22) - (-63) - (-1138) = -1(22) \quad (14)$$

In contrast, reaction 15, discussed earlier,

$$[XeF][AsF_6](s) + AsF_5(l) \rightarrow [XeF][As_2F_{11}](s) \quad (15)$$

is known not to take place. $\Delta G(15)$ is calculated to be

$$\Delta G(15) = \Delta_f G^o([XeF][As_2F_{11}], s) - \Delta_f G^o([XeF][AsF_6], s) - \Delta_f G^o(AsF_5, l) \approx -2339(15) - (-1202(22)) - (-1138) = +1(15)\ \text{kJ mol}^{-1} \quad (16)$$

In the cases of the salts $[XeF_3][AsF_6]$ and $[XeF_3][As_2F_{11}]$ formed by reactions 17 and 18,

$$XeF_4(s) + AsF_5(l) \rightarrow [XeF_3][AsF_6](s) \quad (17)$$

$$XeF_4(s) + 2AsF_5(l) \rightarrow [XeF_3][As_2F_{11}](s) \quad (18)$$

$$\Delta G(17) = \Delta_f G^o([XeF_3][AsF_6], s) - \Delta_f G^o(XeF_4, s) - \Delta_f G^o(AsF_5, l) \approx -1239(26) - (-121) - (-1138) = +20(26)\ \text{kJ mol}^{-1} \quad (19)$$

$$\Delta G(18) = \Delta_f G^o([XeF_3][As_2F_{11}], s) - \Delta_f G^o(XeF_4, s) - 2\Delta_f G^o(AsF_5, l) \approx -2383(15) - (-121) - 2(-1138) = +14(15)\ \text{kJ mol}^{-1} \quad (20)$$

In a paper by Gillespie, Landa, and Schrobilgen,[85] there is reference to an attempt to synthesize $[XeF_3][As_2F_{11}]$ from XeF_4 and excess liquid AsF_5 at −100 °C. The only salt formed in this reaction was $[XeF_3][AsF_6]$ and no evidence for $[XeF_3][As_2F_{11}]$ was reported. Taking account of the calculated errors, $\Delta G(20) = 14 \pm 15$ kJ mol^{-1}, this VBT result could suggest marginal stability. Although evidence is also given in the paper for the formation of $[XeF_3][AsF_6]$, this result also is not in full accord with our result for $\Delta G(17)$ which suggests marginal instability.

Finally, in the above it is assumed that $\Delta_f G^o(AsF_5, l) = -1138$ kJ mol^{-1}, and it is worth considering whether this value is in accord with expected trends. The values of $\Delta_f H^o(SbF_5, l) = -1328$ kJ mol^{-1} and $\Delta_f H^o(SbF_5, g) = -1301$ kJ mol^{-1}[80] correspond to an enthalpy of vaporization of 27 kJ mol^{-1}. Because gaseous SbF_5 is polymeric, and gaseous AsF_5 is monomeric, it may be conjectured that $\Delta_{vap}H^o(AsF_5, l)$ is probably considerably less than $\Delta_{vap}H^o(SbF_5, l)$ at 27 kJ mol^{-1}. This assumption is corroborated by rather approximate relationships both of which do not apply as well for associated liquids and thus probably cannot be expected to well reproduce the data for SbF_5 because of the polymeric nature of the gas. First, Trouton's Rule,[86,87] states that $\Delta_{vap}H^o \approx 88\ T_b$ J mol^{-1}, where T_b is the boiling temperature of the liquid degrees Kelvin. Since T_b for AsF_5 is 220 K and T_b for SbF_5 is 414 K, then Trouton's Rule predicts that $\Delta_{vap}H^o(AsF_5, l) < \Delta_{vap}H^o(SbF_5, l)$, in agreement with our conjecture [with $\Delta_{vap}H^o(SbF_5,l) \approx 36$ kJ mol^{-1} and $\Delta_{vap}H^o(AsF_5,l) \approx 19$ kJ mol^{-1}]. Further indication of the validity of this assumption comes from work by Williams et al.[88] who established the empirical relationship $\Delta_{vap}H^o \approx 0.108\ T_b - 3.99$, having a correlation coefficient $R^2 = 0.99$ and leading to similar values, $\Delta_{vap}H^o(SbF_5,l) \approx 40$ kJ mol^{-1} and $\Delta_{vap}H^o(AsF_5,l) \approx 19$ kJ mol^{-1}.

Thus, $\Delta_f H^o(AsF_5, l)$ lies in the neighborhood of −1191 kJ mol^{-1} because $\Delta_f H^o(AsF_5, g) = -1172$ kJ mol^{-1}.[81] Since $\Delta_f H^o(AsF_5, l) > \Delta_f H^o(SbF_5, l)$, one may also expect that $\Delta_f G^o(AsF_5, l) > \Delta_f G^o(SbF_5, l)$. The adopted value agrees with the latter expectation.

(ii) Predicted Thermochemistry of Krypton Salts using VBT. The existence of a value for $\Delta_f H^o(KrF^+, g)$ allowed the prediction of $\Delta_f H^o$, $\Delta_f S^o$, $\Delta_f G^o$, and S^o_{298} for KrF^+ salts (Table 6). In a critical review,[89] it has been pointed out that, unlike the Xe(II) analogues, all Kr(II) compounds are thermodynamically unstable with respect to redox decomposition. The VBT results in Table 6 bear this out, showing that while $[KrF][SbF_6]$ decomposes according to eq 21 (Ng = Kr):

$$2[NgF][SbF_6](s) \rightarrow [NgF][Sb_2F_{11}](s) + Ng(g) + \tfrac{1}{2}\ F_2(g) \quad (21)$$

for which:

$$\Delta G(21; Ng = Kr) = \Delta_f G^o([KrF][Sb_2F_{11}], s) - 2\Delta_f G^o([KrF][SbF_6], s) \approx -2386(15) - 2(-1134(15)) = -118(26)\ \text{kJ mol}^{-1} \quad (22)$$

the analogous XeF^+ decomposition (eq 21; Ng = Xe) does not occur and is found to be thermodynamically unfavorable:

$$\Delta G(21; Ng = Xe) = \Delta_f G^o([XeF][Sb_2F_{11}], s) - 2\Delta_f G^o([XeF][SbF_6], s) \approx -2618(63) - 2(-1361(52)) = +104(97)\ \text{kJ mol}^{-1} \quad (23)$$

A more extensive comparison of the thermodynamic stabilities of KrF^+ and XeF^+ salts is provided in section (iv) below.

(85) Gillespie, R. J.; Landa, B.; Schrobilgen, G. J. *Inorg. Chem.* **1976**, *15*, 1256–1263.

(86) Trouton, F. *Phil. Mag.* **1884**, *18*, 54–57.

(87) Jenkins, H. D. B. *Chemical Thermodynamics − at a Glance*; Blackwell: Oxford, 2009.

(88) Westwell, M. S.; Searle, M. S.; Wales, D. J.; Williams, D. H. *J. Am. Chem. Soc.* **1995**, *117*, 5013–5015.

(89) Lehmann, J. F.; Mercier, H. P. A.; Schrobilgen, G. J. *Coord. Chem. Rev.* **2002**, *233/234*, 1–39.

(iii) Predicted Thermochemistry of Argon Salts using VBT. There are no reference salts of ArF^+ which can be employed to provide us with an estimate for $V_+(ArF^+)$ to enable VBT data in Table 6 to be estimated. However, by use of volume estimation rules, one can deduce a value, since

$$V_+(MF^+) \approx \tfrac{1}{2}\,[2V_+(M^+) + (V_-(ReF_8{}^{2-}) - V_-(ReF_6{}^{2-})] \quad (24)$$

which, since $V_-(ReF_n{}^{2-}) = 0.149$ nm^3 ($n = 8$) and 0.124 nm^3 ($n = 6$), leads to the relationship

$$V_+(MF^+) \approx V_+(M^+) + 0.013 \quad (25)$$

so that $V_+(MF^+)$ is estimated to be 0.023 (M = K), 0.027 (M = Rb), and 0.032 (M = Cs) nm^3. A linear plot of $V_+(MF^+)$ against the values estimated for $V_+(NgF^+)$, where Ng is chosen as the noble gas adjacent to the alkali metal in the Periodic Table leads to the estimate:

$$V_+(ArF^+) \approx V_+(KF^+) = 0.023\ \text{nm}^3 \quad (26)$$

(average values of $V_+(NgF^+)$ are $V_+(XeF^+) = 0.039(8)$ nm^3 and $V_+(KrF^+) = 0.030(2)$ nm^3; footnote *a* in Table 6). Since $\Delta_f H^o(ArF^+, g)$ is known (1398 kJ mol^{-1}) from the estimated enthalpy for dissociation of $ArF^+(g)$ into $Ar^+(g)$ and F(g),[77] the lattice energy, U_{POT}, for the salt estimated from V_m (Table 6) can be used to estimate $\Delta_f H^o$ for ArF^+ salts.

(iv) VBT Prediction of the Most Plausible ArF^+ Salts and Their Stabilities Compared to Those of Known KrF^+ and XeF^+ Salts. Likely candidates for ArF^+ salts have been the subject of speculation in the literature. Jørgensen[90] suggested that $[ArF]_2[BeF_4]$ and $[ArF][BF_4]$ might be stable while Frenking et al.[77] ruled out the latter salt and laid claim to $[ArF][AuF_6]$ and $[ArF][SbF_6]$ as being the more likely. Liebman and Allen,[91] in a theoretical investigation, further proposed that ArF^+ might be "sufficiently stable to allow the probable isolation of $[ArF^+][PtF_6{}^-]$". They further considered that the factor governing the stabilities of likely salts would be their resistance to "annihilation by F-transfer". The use of an appropriate thermochemical cycle based on reaction 27 affords an analysis of this decomposition route:

$$[ArF][M_mF_{5m+1}](s) \rightarrow Ar(g) + F_2(g) + mMF_5(g) \quad (27)$$

where M = Sb ($m = 1, 2, 3$); M = As, P, Au ($m = 1$) to give

$$\Delta H(27) = U_{POT}([ArF][M_mF_{5m+1}]) + {}^3/_2\,RT - FIA(mMF_5, g) - \Delta_f H^o(ArF^+, g) - \Delta_f H^o(F^-, g)$$
$$= U_{POT}([ArF][M_mF_{5m+1}]) + {}^3/_2\,RT - FIA(mMF_5, g) = -1141\ \text{kJ mol}^{-1} \quad (28)$$

(90) Jørgensen, C. K. *Z. Anorg. Allg. Chem.* **1986**, *540*, 91–105.
(91) Liebman, J.; Allen, L. C. *J. Chem. Soc., Chem. Commun.* **1969**, 1355.

while the corresponding entropy change for eq 27 is

$$\Delta S(27) = S^o{}_{298}(Ar, g) + S^o{}_{298}(F_2, g) + mS^o{}_{298}(MF_5, g) - S^o{}_{298}([ArF][M_mF_{5m+1}]) \quad (29)$$

In order that $\Delta H(27) > 0$ (representing a resistance to decomposition and hence thermodynamic stability), $U_{POT}([ArF][M_mF_{5m+1}])$ needs to be high and thus $V_-(M_mF_{5m+1}{}^-)$ small. The FIA for m moles of $MF_5(g)$ (defined as $mMF_5(g) + F^-(g) \rightarrow M_mF_{5m+1}{}^+(g)$) will need to be as low (numerically) as possible.

$$\Delta S(27) = 343 + mS^o{}_{298}(MF_5, g) - 1360V_m([ArF][M_mF_{5m+1}]) \quad (30)$$

The values estimated by VBT for all the ArF^+ salts for $\Delta H(27)$, $\Delta S(27)$, and $\Delta G(27)$, for the cases where M = Sb ($m = 1, 2, 3$) and M = As, P, Au ($m = 1$) are as follows:

$[ArF][SbF_6]$: $\Delta H(27) \approx 80(64)$ kJ mol^{-1}; $\Delta S(27) \approx 501$ J K^{-1} mol^{-1}; $\Delta G(27) \approx -229(64)$ kJ mol^{-1}

$[ArF][Sb_2F_{11}]$: $\Delta H(27) \approx 10(64)$ kJ mol^{-1}; $\Delta S(27) \approx 712$ J K^{-1} mol^{-1}; $\Delta G(27) \approx -202(64)$ kJ mol^{-1}

$[ArF][Sb_3F_{16}]$: $\Delta H(27) \approx 31(39)$ kJ mol^{-1}; $\Delta S(27) \approx 943$ J K^{-1} mol^{-1}; $\Delta G(27) \approx -250(39)$ kJ mol^{-1}

$[ArF][AsF_6]$: $\Delta H(27) \approx -153(23)$ kJ mol^{-1}; $\Delta S(27) \approx 502$ J K^{-1} mol^{-1}; $\Delta G(27) \approx -303(23)$ kJ mol^{-1}

$[ArF][PF_6]$: $\Delta H(27) \approx -176$ kJ mol^{-1}; $\Delta S(27) \approx 451$ J K^{-1} mol^{-1}; $\Delta G(27) \approx -310$ kJ mol^{-1}

$[ArF][AuF_6]$: $\Delta H(27) \approx 73(65)$ kJ mol^{-1}; $\Delta S(27) \approx 508$ J K^{-1} mol^{-1}; $\Delta G(27) \approx -224(65)$ kJ mol^{-1}

All the above ArF^+ salts are then predicted to decompose according to eq 27. Where analysis, based solely on the

enthalpy term, $\Delta H(27)$, appears to favor stability, in every case the magnitude of the entropy term, $-T\Delta S(27)$, confers instability.

Using the analogous decompositions according to eq 27 for the KrF^+ and XeF^+ salts, the following VBT data result:

$$[KrF][SbF_6]: \Delta H(27) \approx 45 \text{ kJ mol}^{-1}$$
$$\Delta S(27) \approx 504 \text{ J K}^{-1} \text{ mol}^{-1}$$
$$\Delta G(27) \approx -105 \text{ kJ mol}^{-1}$$

$$[KrF][Sb_2F_{11}]: \Delta H(27) \approx 137 \text{ kJ mol}^{-1}$$
$$\Delta S(27) \approx 711 \text{ J K}^{-1} \text{ mol}^{-1}$$
$$\Delta G(27) \approx -75 \text{ kJ mol}^{-1}$$

$$[KrF][AsF_6]: \Delta H(27) \approx -30 \text{ kJ mol}^{-1}$$
$$\Delta S(27) \approx 503 \text{ J K}^{-1} \text{ mol}^{-1}$$
$$\Delta G(27) \approx -180 \text{ kJ mol}^{-1}$$

$$[KrF][PF_6]: \Delta H(27) \approx -29 \text{ kJ mol}^{-1}$$
$$\Delta S(27) \approx 448 \text{ J K}^{-1} \text{ mol}^{-1}$$
$$\Delta G(27) \approx -163 \text{ kJ mol}^{-1}$$

$$[KrF][AuF_6]: \Delta H(27) \approx 48 \text{ kJ mol}^{-1}$$
$$\Delta S(27) \approx 506 \text{ J K}^{-1} \text{ mol}^{-1}$$
$$\Delta G(27) \approx -103 \text{ kJ mol}^{-1}$$

$$[XeF][SbF_6]: \Delta H(27) \approx 240 \text{ kJ mol}^{-1}$$
$$\Delta S(27) \approx 495 \text{ J K}^{-1} \text{ mol}^{-1}$$
$$\Delta G(27) \approx +92 \text{ kJ mol}^{-1}$$

$$[XeF][Sb_2F_{11}]: \Delta H(27) \approx 339 \text{ kJ mol}^{-1}$$
$$\Delta S(27) \approx 709 \text{ J K}^{-1} \text{ mol}^{-1}$$
$$\Delta G(27) \approx +128 \text{ kJ mol}^{-1}$$

$$[XeF][AsF_6]: \Delta H(27) \approx 165 \text{ kJ mol}^{-1}$$
$$\Delta S(27) \approx 494 \text{ J K}^{-1} \text{ mol}^{-1}$$
$$\Delta G(27) \approx +18 \text{ kJ mol}^{-1}$$

$$[XeF][PF_6]: \Delta H(27) \approx 127 \text{ kJ mol}^{-1}$$
$$\Delta S(27) \approx 449 \text{ J K}^{-1} \text{ mol}^{-1}$$
$$\Delta G(27) \approx -7 \text{ kJ mol}^{-1}$$

The last result is somewhat anomalous, but the uncertainties are such that to claim $[XeF][PF_6]$ behaves differently to the other XeF^+ salts with respect to stability would be unwarranted.

The VBT analyses conclude that the hypothetical ArF^+ salts are thermodynamically unstable with respect to F_2 gas and gaseous pentafluoride formation for the aforementioned choices of element M of the anion. The VBT results are in full accord with the known thermochemical stabilities of XeF^+ salts and the relative instabilities of KrF^+ salts.

(v) Typical $\Delta_f H^o$, $\Delta_f G^o$, and S^o_{298} Values for ArF^+ Salts. So far, $\Delta_f H^o([XeF][SbF_6], s) = -1568(52)$ kJ mol^{-1} has been estimated (Table 6, column 10), which is in close agreement with the experimental value, -1523 kJ mol^{-1}, and $\Delta_f G^o([XeF][SbF_6], s)$ is predicted to be $-1361(52)$ kJ mol^{-1}, with the two values differing by 207 kJ mol^{-1}. Correspondingly, for $[KrF][SbF_6]$: $\Delta_f H^o([KrF][SbF_6], s) = -1342$ kJ mol^{-1} and $\Delta_f G^o([KrF][SbF_6], s) = -1134$ kJ mol^{-1}, which differ by 208 kJ mol^{-1}. For further comparison, the values for the hypothetical salt (being unstable with respect to Ar(g), F_2(g), and SbF_5(g)), $[ArF][SbF_6]$, are derived

$$\Delta_f H^o([ArF][SbF_6], s) = \Delta_f H^o(ArF^+, g) + \Delta_f H^o(SbF_6^-, g) - U_{POT}([ArF][SbF_6]) - {}^3/_2\, RT$$
$$\approx 1398 + (-2076(52)) - 3.7 - U_{POT}([ArF][SbF_6]) \quad (31)$$

Since VBT predicts that $U_{POT}([ArF][SbF_6]) = 551$ (11) kJ mol^{-1},

$$\Delta_f H^o([ArF][SbF_6], s) \approx -1232(53) \text{ kJ mol}^{-1} \quad (32)$$

and since, $V_m([ArF][SbF_6]) = 0.144(12)$ nm^3

$$S^o_{298} = 1360 V_m([ArF][SbF_6]) + 15$$
$$\approx 211 \text{ J K}^{-1} \text{ mol}^{-1} \quad (33)$$

so that

$$\Delta_f S^o_{298}([ArF][SbF_6], s) \approx S^o_{298}([ArF][SbF_6]) - S^o_{298}(Ar, g) - S^o_{298}(Sb, s) - {}^7/_2 S^o_{298}(F_2, g) \approx 211 - 154.8 - 45.7 - 709.7 \approx -699 \text{ J K}^{-1} \text{ mol}^{-1} \quad (34)$$

giving

$$\Delta_f G^o([ArF][SbF_6], s) \approx -1024(53) \text{ kJ mol}^{-1} \quad (35)$$

Here again, the difference, $\Delta_f H^o - \Delta_f G^o$, is 208 kJ mol^{-1}. Although this constant difference is not imposed on these SbF_6^- noble-gas salts by any assumptions that have been made, and it also appears that BF_4^- and $Sb_2F_{11}^-$ salts of NgF^+ cations exhibit differences of ~154 and 328 kJ mol^{-1}, respectively, this relationship does not appear to apply more generally to other anions.

Conclusion

The crystal structures of $[XeF][SbF_6]$, $[XeF][BiF_6]$, and $[XeF][Bi_2F_{11}]$ have been determined for the first time and the crystal structures of XeF_2, $[XeF][AsF_6]$, $[XeF][Sb_2F_{11}]$, and $[XeF_3][Sb_2F_{11}]$ have been redetermined with greater precision at −173 °C. Despite significant variations among the FIAs of the parent pnictogen pentafluorides, the $Xe-F_t$ bond lengths of the XeF^+ salts do not differ significantly among the structures of $[XeF][MF_6]$ (M = As, Sb) and $[XeF][Sb_2F_{11}]$. With the exception of $[XeF][BiF_6]$ and $[XeF][Bi_2F_{11}]$, where the $Xe-F_t$ bond lengths are slightly longer, this trend is consistent with the absence of significant $Kr-F_t$ bond length variations among the structures of the $[KrF][MF_6]$ (M = As, Sb, Bi, Au) salts. The experimental $Ng---F_b$ bond lengths of the $[NgF][MF_6]$ salts show greater anion dependencies than the $Ng-F_t$ bonds. The $Xe-F_t$ bond lengths increase in the order $[XeF][BiF_6] \approx [XeF][AsF_6] < [XeF][Bi_2F_{11}] < [XeF][SbF_6] < [XeF][Sb_2F_{11}]$, whereas the $Kr-F_t$ bond lengths increase in the order $[KrF][BiF_6] < [KrF][AsF_6] < [KrF][SbF_6]$. Overall, this ordering is consistent with the relative FIAs of the parent MF_5 (M = As, Sb, Bi) and M_2F_{10} (M = Sb, Bi) Lewis acids with the exception of BiF_6^- and $Bi_2F_{11}^-$ which interact more strongly with XeF^+ than predicted from the FIAs of their parent Lewis acids, BiF_5 and Bi_2F_{10}.

The calculated gas-phase geometries of the $[NgF][MF_6]$ ion pairs are compared with the crystal structures. The optimized geometries of the $[NgF][MF_6]$ ion pairs all have staggered conformations, whereas only $[XeF][AsF_6]$ displays a staggered geometry in its crystal structure. The vibrational spectra obtained from these energy-minimized structures were used to reinterpret the spectra of the $[NgF][MF_6]$ (M = As, Sb, Bi) salts in greater detail. Reasonable agreement was obtained for the $Ng-F_t$ stretching frequencies; however, the calculations showed that the $Ng---F_b$ and $M---F_b$ stretches are in-phase and out-of-phase coupled. The NBO analyses of calculated structures indicate that the $[XeF][MF_6]$ salts are more ionic than their krypton analogues, attesting to the greater fluoride ion donor strength of XeF_2 relative to that of KrF_2.

The thermochemistry section of this paper has illustrated uses of VBT in noble-gas chemistry where experimental thermodynamic information is limited. Its application, while leading to approximate thermodynamic parameters, provides a valuable predictive tool. The VBT approach provides a link between (crystal) structural features through volume and lattice energy and the corresponding thermochemistry for crystalline materials. In the few situations where thermochemical facts are known, VBT tends to validate and confirm these, giving some confidence that in predictive mode the results should provide a guide to thermodynamic possibilities. Despite a general paucity of thermochemical data, VBT on the whole is able to provide estimates and predict stabilities, albeit sometimes with quite large uncertainties in the estimated data. While the stabilities of $[XeF_n][Sb_2F_{11}]$ (n = 2, 3) and $[XeF][AsF_6]$ are confirmed with respect to dissociation to the xenon fluoride and pnictogen pentafluoride, the stabilities of $[XeF_3][AsF_6]$ and $[XeF_3][As_2F_{11}]$ are shown to be marginal under standard conditions. VBT, inter alia, confirms that the known XeF^+ salts are thermodynamically stable with respect to redox decomposition and that KrF^+ salts and all (hypothetical) ArF^+ salts considered are unstable with respect to redox decomposition to Ng(g), F_2(g), and MF_5(g) (Ng = Ar, Kr; M = Sb, As, P, and Au). VBT is extremely simple to use and can be used by non-experts. Those wishing to learn more should consult the Supporting Information and references therein.

Experimental Section

Apparatus and Materials. All manipulations involving air-sensitive materials were carried out under strictly anhydrous conditions as previously described.[92] Volatile materials were handled in vacuum lines constructed of stainless steel, nickel and FEP fluoroplastic, and nonvolatile materials were handled in the dry nitrogen atmosphere of a glovebox. Reaction vessels/Raman sample tubes were fabricated from $^1/_4$-in. o.d. FEP tubing and outfitted with Kel-F valves. Crystallizations in aHF were carried out in T-shaped reaction vessels comprised of $^1/_4$-in. o.d. FEP vessels having $^1/_4$-in. o.d. side arms fused at right angles about two-thirds of the distance from the bottom of the reaction vessel. All reaction vessels and sample tubes were rigorously dried under dynamic vacuum prior to passivation with 1 atm of F_2 gas.

Xenon difluoride was prepared as described in the literature[93] by reacting F_2 with a 2-fold excess of xenon in a nickel can at 400 °C for 7 h. Arsenic pentafluoride was prepared as previously described[94] and was used without further purification. Anhydrous HF (Harshaw Chemical Co.),[95] SbF_3 (Aldrich, 98%),[92] and BiF_5 (Ozark Mahoning Co.)[22] were purified by the standard literature methods. Purified HF was stored over BiF_5 in a Kel-F vessel equipped with a Kel-F valve until used. Fluorine gas (Air Products) was used without further purification. Antimony pentafluoride used in the preparation of $[XeF][SbF_6]$ was synthesized in situ by direct fluorination of SbF_3 with F_2 in anhydrous HF as previously described.[92] Antimony pentafluoride (Ozark Mahoning) used in the preparation of $[XeF][Sb_2F_{11}]$ was purified by distillation as previously described.[96]

Syntheses and Crystal Growth. (a) $[XeF][MF_6]$. The salt, $[XeF][AsF_6]$, was prepared by condensing a 25% stoichiometric excess of AsF_5 (0.177 mmol) onto a frozen solution of 24.0 mg (0.142 mmol) of XeF_2 in ca. 0.5 mL of aHF at −196 °C. After warming to ambient temperature and thorough mixing, the excess AsF_5 and HF were removed under vacuum at −78 °C. Crystals of $[XeF][AsF_6]$ were obtained by allowing the material to sublime in the FEP reactor under a nitrogen atmosphere over the course of several months.

Xenon difluoride (31.5 mg, 0.187 mmol) was transferred, inside a drybox to a frozen HF solution of SbF_5 (42.0 mg, 0.194 mmol) contained in a $^1/_4$ in o.d. FEP T-shaped reactor fitted with a Kel-F valve. The SbF_5 solution had been prepared by distilling ca. 0.5 mL onto 34.8 mg (0.194 mmol) of SbF_3 followed by the addition of 1000 Torr of F_2 every ½ h for 1 ½ h. The resulting SbF_5 was in slight excess (3.6% mol) relative to XeF_2. The reactor was removed from the drybox and allowed to warm to room temperature for the reaction to take place.

Xenon difluoride (10.6 mg, 0.0806 mmol) and BiF_5 (25.4 mg, 0.0832 mmol) were added to an FEP T-shaped reactor inside a drybox. The reactor and contents were removed from the drybox and about 0,5 mL of aHF was condensed onto the mixture at −196 °C and then allowed to warm to room temperature for reaction to take place.

(92) Casteel, W. J., Jr.; Dixon, D. A.; Mercier, H. P. A.; Schrobilgen, G. J. *Inorg. Chem.* **1996**, *35*, 4310–4322.
(93) Mercier, H. P. A.; Sanders, J. C. P.; Schrobilgen, G. J.; Tsai, S. *Inorg. Chem.* **1993**, *32*, 386–393.
(94) Emara, A. A. A.; Lehmann, J. F.; Schrobilgen, G. J. *J. Fluorine Chem.* **2005**, *126*, 1373–1376.
(95) Emara, A. A. A.; Schrobilgen, G. J. *Inorg. Chem.* **1992**, *31*, 1323–1332.
(96) Gillespie, R. J.; Netzer, A.; Schrobilgen, G. J. *Inorg. Chem.* **1974**, *13*, 1455–1459.

Crystals of the $[XeF][AsF_6]$ and $[XeF][SbF_6]$ were grown as previously described[1,2] by slowly cooling the HF solutions over the course of several hours from ca. 0 to −78 °C. The HF and excess pentafluoride were then decanted into the side arm of the vessel which was then cooled and sealed off under vacuum. The crystals were then stored under an atmosphere of dry nitrogen.

(b) $[XeF][Sb_2F_{11}]$. Inside the drybox, 250 mg (0.148 mmol) of XeF_2 was loaded into a FEP and SbF_5 (1.0 mL, 1.4 mmol) was distilled on top of the XeF_2 at −196 °C. The reactor was initially warmed to room temperature and then to 60 °C to ensure that the reaction was complete. The resulting bright yellow solution was allowed to slowly cool to room temperature over the course of 2 days in a well insulated water bath to slow the crystallization of $[XeF][Sb_2F_{11}]$. The excess SbF_5 was removed under dynamic vacuum, and the crystalline product was stored under dry nitrogen.

(c) $[XeF][Bi_2F_{11}]$. Xenon difluoride (6.50 mg, 0.0386 mmol) and BiF_5 (23.5 mg, 0.0965 mmol) were added to an FEP T-reactor in the drybox. The reactor and contents were removed from the drybox, and aHF was condensed onto the mixture at −196 °C and then allowed to warm to room temperature for the reaction to take place. Crystals were grown from the solution by slow removal of the solvent under dynamic vacuum at −48 °C.

(d) Attempts to Synthesize $[XeF][As_2F_{11}]$. Approximately 565 mg (3.33 mmol) of AsF_5 was condensed onto 75.4 mg (0.222 mmol) of $[XeF][AsF_6]$ in a FEP reaction vessel. Liquid AsF_5 and $[XeF][AsF_6]$ were warmed to −78 °C and allowed to react for 24 h. The Raman spectrum of the XeF^+ salt was recorded under frozen AsF_5 at −160 °C and shown to be $[XeF][AsF_6]$ in admixture with solid AsF_5. The procedure was repeated after allowing the sample to stand at −30 °C for 3 h and again was shown to yield a mixture of $[XeF][AsF_6]$ and AsF_5 when the Raman spectrum was recorded at −160 °C. An attempt to grow crystals of $[XeF][As_2F_{11}]$ entailed condensing about 0.2 mL of HF onto the aforementioned mixture at −196 °C, followed by warming to room temperature to effect dissolution of $[XeF][AsF_6]$. Slow cooling of the solution from −40 to −78 °C only yielded crystalline $[XeF][AsF_6]$, which was again verified by recording the Raman spectrum of the frozen sample at −160 °C.

X-ray Crystallography. (a) Collection and Reduction of X-ray Data. The crystal used in this study had the following characteristics: XeF_2 ($0.14 \times 0.08 \times 0.08$ mm^3, wedge), $[XeF][AsF_6]$ ($0.18 \times 0.08 \times 0.08$ mm^3, needle, colorless), $[XeF][SbF_6]$ ($0.20 \times 0.06 \times 0.06$ mm^3, needle, colorless), $[XeF][BiF_6]$ ($0.20 \times 0.04 \times 0.02$ mm^3, thin plate, colorless), $[XeF][Sb_2F_{11}]$ ($0.20 \times 0.08 \times 0.08$ mm^3, needle, pale yellow), $[XeF][Bi_2F_{11}]$ ($0.12 \times 0.04 \times 0.04$ mm^3, needle, pale yellow), and $[XeF_3][Sb_2F_{11}]$ ($0.12 \times 0.08 \times 0.02$ mm^3, plate, pale yellow). The crystals were mounted on glass pins using Fomblin polyether oils as adhesives at -110 ± 5 °C as previously described.[97] The crystals were then centered on a P4 Siemens diffractometer, equipped with a Siemens SMART 1K CCD area detector, controlled by SMART,[98] and a rotating anode emitting Kα radiation monochromated ($\lambda = 0.71073$ A) by a graphite crystal. The distance between the crystal and the detector face was typically 5 cm, and the collection of data was performed using 512×512 pixel modes using 2×2 pixel binning. The raw diffraction data was integrated in three dimensions using SAINT+,[98] which applied Lorentz and polarization corrections to the integrated spot intensities. Scaling of the integrated data was performed with SADABS,[99] which applied decay corrections and an empirical absorption correction on the basis of the intensity ratios of redundant reflections.

(b). Solution and Refinement of the Structure. The program XPREP[100] was used to confirm the unit cell dimensions and the crystal lattices. A solution was found using direct methods to determine the locations of the heavy elements (Xe, As, Sb, Bi). The fluorine positions were identified in successive difference Fourier syntheses. Final refinements were obtained by introducing anisotropic parameters for all the atoms, an extinction parameter, and the recommended weight factor. The maximum electron densities in the final difference Fourier maps were located around the heavy atoms.

Raman Spectroscopy. Raman spectra of $[XeF][MF_6]$ (M = As, Sb) were obtained that were of better quality than those previously published.[21] The spectra were recorded on a Bruker RFS 100 FT-Raman spectrometer at −163 °C using 1064-nm excitation. Between 300 and 500 scans were accumulated at a laser power of 300 mW and 1 cm^{-1} resolution as previously described.[97]

Computational Methods. The optimized geometries and frequencies of $[NgF][MF_6]$ (Ng = Kr, Xe; M = As, Sb, Bi) were calculated at the PBE1PBE, SVWN, B3LYP, MPW1PW91, and MP2 levels of theory using cc-pVTZ, aug-cc-pVDZ, aug-cc-pVTZ or aug-cc-pVQZ for all atoms.[101] Pseudopotentials were used with the appropriate basis sets for Kr, Xe, As, Sb, Bi (cc-pVTZ, aug-cc-pVDZ, aug-cc-pVTZ, aug-cc-pVQZ). The combined use of cc-pVTZ, aug-cc-pVDZ, aug-cc-pVTZ, aug-cc-pVQZ and cc-pVTZ-PP, aug-cc-pVDZ-PP, aug-cc-pVTZ-PP, aug-cc-pVQZ-PP basis sets, respectively, is indicated as cc-pVTZ(-PP), aug-cc-pVDZ(-PP), aug-cc-pVTZ(-PP) and aug-cc-pVQZ(-PP).[101] The NBO analyses[49−52] were performed for the PBE1PBE/aug-cc-pVQZ(-PP) optimized local minima. Quantum-chemical calculations were carried out using the program Gaussian 09[102] for geometry optimizations, vibrational frequencies, and their intensities and the program Gaussian 03[103] for NBO analysis. The program GaussView[104] was used to visualize the vibrational displacements that form the basis for the vibrational mode descriptions given in Table 4, and Supporting Information, Tables S2 and S4−S6.

Acknowledgment. We thank the Natural Sciences and Engineering Research Council of Canada for the award of a postgraduate scholarship and McMaster University for a Dalley Fellowship (J.F.L.) and for support in the form of a Discovery Grant (G.J.S.); and SHARCNet (Shared Hierarchical Academic Research Computing Network; www.sharcnet.ca) for computational resources. Special thanks are accorded to David S. Brock who investigated the low-temperature reactions between excess AsF_5 and $[XeF][AsF_6]$.

Supporting Information Available: Packing diagram of XeF_2 (Figure S1); additional experimental and calculated geometrical parameters (Table S1) and vibrational frequencies (Table S2) for $[XeF][MF_6]$ (M = As, Sb, Bi); experimental and calculated geometrical parameters (Table S3) and vibrational frequencies (Tables S4−S6) for $[KrF][MF_6]$ (M = As, Sb, Bi); calculated

(97) Gerken, M.; Schrobilgen, G. J. *Inorg. Chem.* **2000**, *39*, 4244–4255.
(98) *SMART, release 5.611, and SAINT, release 6.02*; Siemens Energy and Automotive Analytical Instrumentation, Inc.: Madison, WI, 1999.
(99) Sheldrick, G. M. *SADABS* (*Siemens Area Detector Absorption Corrections*), version 2.03; Madison, WI, 1999.
(100) Sheldrick, G. M. *SHELXTL-Plus*, release 5.1; Siemens Analytical X-ray Instruments, Inc.: Madison, WI, 1998.
(101) Basis sets were obtained from the Extensible Computational Chemistry Environment Basis set Database, version 2/25/04, as developed and distributed by the Molecular Science Computing Facility, Environmental and Molecular Science Laboratory, which is part of the Pacific Northwest Laboratory, P.O. Box 999, Richland, WA 99352.
(102) Frisch, M. J.; et al. *Gaussian 09*, revision A.02; Gaussian, Inc.: Wallingford, CT, 2009.
(103) Frisch, M. J.; et al. *Gaussian 03*, revision D.01; Gaussian, Inc.: Wallingford, CT, 2004.
(104) *GaussView*, release 3.0; Gaussian Inc.: Pittsburgh, PA, 2003.

geometry of $[XeF][BiF_6]$ (Figure S2); NBO analysis for $[KrF][MF_6]$ (M = As, Sb, Bi) (Table S7); synthesis and low-temperature X-ray crystal structure of $[XeF_3][Sb_2F_{11}]$; complete references 102 and 103; background on the thermochemical study of noble-gas fluorocation salts; flowchart showing the use of VBT (Figure S3); additional references. X-ray crystallographic file in CIF format for the structure determination of $[XeF][MF_6]$ (M = As, Sb, Bi), $[XeF][M_2F_{11}]$ (M = Sb, Bi) and $[XeF_3][Sb_2F_{11}]$. This material is available free of charge via the Internet at http://pubs.acs.org.